

POPULATION STRUCTURE OF CHUB MACKEREL (*SCOMBER COLIAS*) IN THE NORTHEAST ATLANTIC INFERRED FROM NATURAL TAGS

Alessandra Alves Muniz

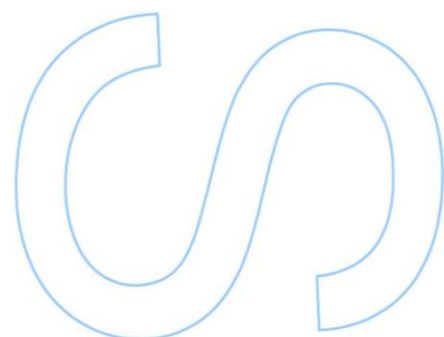
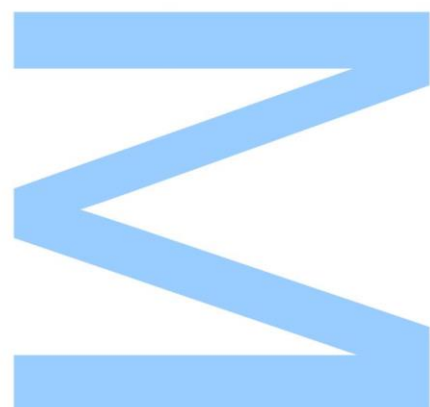
Mestrado em Ciências e Tecnologia do Ambiente – Área de
especialização em Riscos: Avaliação e Gestão de Risco
Departamento de Geociências, Ambiente e Ordenamento do Território
2018

Supervisor

Alberto Teodorico Correia, Professor Auxiliar, Faculdade de Ciências da
Saúde da Universidade Fernando Pessoa e Centro Interdisciplinar de
Investigação Marinha e Ambiental

Co-supervisor

Paulo Talhadas dos Santos, Professor Auxiliar, Faculdade de Ciências da
Universidade do Porto



This work has been already presented in three international congresses:

Muniz AA, Moura A, Triay-Portella R, Moreira C, Santos PT, Correia AT. 2018. Stock discrimination of Chub Mackerel (*Scomber colias*) in the NE Atlantic inferred from body morphometric. IMMR'18. 05-06 July. Peniche. Portugal. Poster

Muniz AA, Moura A, Triay-Portella R, Santos PT, Pinto E, Almeida A, Correia AT. 2018. Biogeochemical signatures of otoliths as a tool to study the population structure, movement and habitat connectivity of Chub Mackerel (*Scomber colias*) in the Northeast Atlantic. SIBIC VII. 12-15 June. Faro. Portugal. Oral.

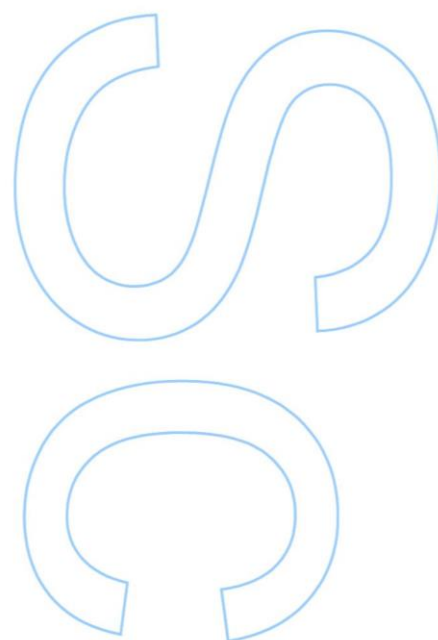
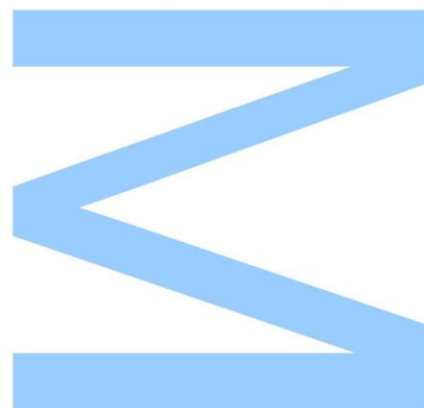
Muniz AA, Moura A, Triay-Portella R, Santos PT, Correia AT. 2018. Population structure of Chub Mackerel (*Scomber colias*) in the Northeast Atlantic inferred from otolith shape analysis. SIBIC VII. 12-15 June. Faro. Portugal. Poster



Todas as correções determinadas
pelo júri, e só essas, foram efetuadas.

O Presidente do Júri,

Porto, ____/____/____



Acknowledgements

My sincere thanks to my supervisor, Professor Alberto Teodorico Correia, for the opportunity, for your attention, patient, teachings and never denning to help me. The confidence you deposited in me and all the incentive was essential for my academic maturity. It was great working with you and I hope to have the good fortune to meet you again on future projects. Professor Paulo Talhadas dos Santos, thank you for accepting the co-supervision.

Thank you to all colleagues in CIIMAR Ecophysiology Group for coexistence and good relationships. Specially, to my friend, Ana Moura, for the help in all the steps of this work, for the company, partnership, good memories and friendship that I will bring to life. Special thanks to Paulo Castro (IPMA - Matosinhos), Artur Gomes (Lota - Sesimbra), Carolino Rodrigues (Lota - Portimão), Graça Faria and João Delgado (DRP - Madeira) for fish acquisition, and to Cláudia Moreira, Raül Triay-Portella, Edgar Pinto and Agostinho Almeida for all contributions in this work.

I am so thankful God for providing me a wonderful family with an unconditional love that has kept me strong throughout my journey so far from home. Specially, to my parents, José Muniz and Sandra Muniz, for the entire base that shaped me, with the confidence that they are proud of me. To my sister, Elizandra Muniz, thank you for the partnership, and for being my example of person and professional. To my fiancé, Victor Alves, thank you for accompanying me during this stage, for the support and daily encouragement and for being companionship, always, in all the challenges and difficult moments. To all my friends in Brazil and to those I met in Portugal, the good moments of relaxation and lightness were essential to recharge forces during the stages of work.

Abstract

Atlantic chub mackerel (*Scomber colias*) is one of the main pelagic fisheries resources in the NE Atlantic. Commercial landings of *S. colias* have increased significantly in the Iberian Peninsula, in both Portugal and Spain, during the last years. At present, and for fisheries management purposes, we consider the existence of a single stock of this species in the NE Atlantic. However, the information regarding the population structure of this species is still limited. Juveniles collected from Portugal mainland (Portimão, Sesimbra, Matosinhos) and the Atlantic oceanic Islands (Azores, Canaries and Madeira) from January to April 2018 were used. Following age estimation by counting the annual growth increments of sagittae, pre-selected individuals of the same age group (2 years old) were used for body morphometric and otolith shape analyses (45 fish per location), and for otolith chemical signatures (30 fish per location). Data were analysed by univariate and multivariate statistics to assess the degree of separation between the individuals of these geographic regions. Data showed regional differences in the otolith shape analysis, body morphometric, and otolith fingerprinting. Reclassification success using shape analysis, body morphometric and otolith fingerprinting showed an overall rate of 51%, 74% and 78%, respectively. Regional differences regarding the otolith shape were mainly drive by EL, RE, RO, A2, A3, B5, D2, D3 and D5, showing the existence of two main groups (oceanic islands and Portugal mainland). Concerning body morphometric, regional differences were mainly drive by distances 1, 2, 3, 8, 9, 11, 14, 19, 22 and 26, showing a separation of the three main groups (Canaries, Azores/Madeira and Portugal mainland). Finally, for the otolith fingerprints, regional differences were mainly drive by Sr:Ca, Li:Ca, Mn:Ca, Mg:Ca, Rb:Ca, Ba:Ca, $\delta^{13}\text{C}$ and $\delta^{18}\text{O}$, showing a clear separation of the four main sampling regions (Canaries, Azores, Madeira and Portugal mainland), providing support for treatment of these fisheries as different management units.

Key-words: pelagic fish, stock delineation, otolith shape, body morphometric, otolith fingerprinting.

Resumo

A cavala do Atlântico (*Scomber colias*) é um dos principais recursos de pesca pelágica no Atlântico NE. Os desembarques comerciais de *S. colias* aumentaram significativamente na Península Ibérica nos últimos anos, quer em Portugal, quer em Espanha. No Atlântico NE considera-se atualmente a existência de uma única unidade populacional para fins de manejo pesqueiro. No entanto, as informações sobre a estrutura populacional desta espécie, no momento, ainda são limitadas. Juvenis foram coletados em Portugal continental (Portimão, Sesimbra e Matosinhos) e nas ilhas do oceano Atlântico (Açores, Canárias, Madeira) de janeiro a abril de 2018. Após uma estimativa de idade com recurso à contagem dos incrementos anuais de crescimento dos sagittae, indivíduos pré-selecionados do mesmo grupo etário (2 anos de idade) foram usados para análise da morfometria corporal e da forma do otólito (45 peixes por local), bem como para a análise da assinatura química do otólito (30 peixes por local). Os dados foram analisados através de estatística univariada e multivariada para avaliar o grau de separação entre os indivíduos destas regiões geográficas. Os resultados mostraram diferenças regionais na análise da forma do otólito, morfometria corporal e assinatura química dos otólitos. A taxa de reclassificação global usando análise de forma dos otólitos, morfometria corporal e assinatura química dos otólitos foi de 51%, 74% e 78%, respectivamente. Diferenças regionais obtidas considerando apenas a forma do otólito foram impulsionadas principalmente por EL, RE, RO, A2, A3, B5, D2, D3 e D5, mostraram a existência de dois principais grupos (Ilhas Oceânicas e Portugal Continental). No caso da morfometria corporal as diferenças regionais foram resultado sobretudo das distâncias 1, 2, 3, 8, 9, 11, 14, 19, 22 e 26, mostrando a separação de em três principais grupos (Canárias, Açores/Madeira e Portugal Continental). Finalmente, no caso da química dos otólitos, as diferenças regionais químicas foram fruto principalmente das relações Sr:Ca, Li:Ca, Mn:Ca, Mg:Ca, Rb:Ca, Ba:Ca, $\delta^{13}\text{C}$ e $\delta^{18}\text{O}$, mostrando uma separação clara em quatro grupos (Canárias, Açores, Madeira e Portugal Continental), sugerindo que na gestão deste recurso pesqueiro estas regiões sejam consideradas diferentes unidades populacionais.

Palavras-chave: Peixe pelágico, delineação do estoque, forma do otólito, morfometria corporal, assinaturas químicas do otólito.

Índex

Acknowledgements	i
Abstract	ii
Resumo	iii
1. INTRODUCTION	1
1.1 Ecology	2
1.2 Spacial distribution and landings	4
1.3 Natural tags	6
2. OBJECTIVES	8
2.1 General Objective	8
2.2 Specific Objectives	8
3. MATERIALS AND METHODS	9
3.1 Samples collection	9
3.1.1 Age estimates	11
3.2 Body morphometric	13
3.2.1 Statistical Analysis	15
3.3 Otolith shape analysis	16
3.3.1 Statistical Analysis	18
3.4 Otolith Chemistry Analysis	18
3.4.1 Elemental Signatures	19
3.4.2 Isotopic Signatures	20
3.4.3 Statistical Analysis	20
4. RESULTS	22
4.1 Body morphometrics	22
4.2 Otolith Shape	25
4.3 Otolith Chemistry	31
5. DISCUSSION	37
6. CONCLUSION	42
7. FINANTIAL SUPPORT	43
8. REFERENCES	44

Índex of Figures

Figure 1: A <i>S. colias</i> specimen (23,4 cm of total length) collected in Portimão in February 2018 (personal photograph).	2
Figure 2: Distribution range colours indicate degree of suitability of habitat which can be interpreted as probabilities of occurrence of the <i>Scomber colias</i> . Source: Aquamaps. 2016. Reviewed Native Distribution Map for <i>Scomber colias</i> (Atlantic chub mackerel), with modelled year 2100 native range map based on IPCC A2 emissions scenario. www.aquamaps.org, version of Aug. 2016. Web. Accessed 4 Jun. 2018.	5
Figure 3: Sampling locations of <i>Scomber colias</i> caught in the NE Atlantic from January to April 2018.	10
Figure 4: <i>S. colias</i> collected in Matosinhos in the January 2018 (personal photograph).	10
Figure 5: Otoliths of <i>Scomber colias</i> (23,1 cm of total length) collected in Sesimbra in 2018 (personal captation).	13
Figure 6: Locations of the 13 selected landmarks on the fish left side (adapted from Collette, 1986).	14
Figure 7: <i>Scomber colias</i> collected from Azores in February 2018 (26,8 cm of total length) showing the body landmarks (personal photograph).	15
Figure 8: Right otolith sagittal photograph of the <i>Scomber colias</i> and the corresponding binary digital image, respectively.	16
Figure 9: Contour otolith shape of 1 Principal component (23% significance cumulative) of 20 Principal components (95% significance cumulative) (Output EFD).	17
Figure 10: Canonical variable plots show differences for body morphometric of <i>Scomber colias</i> for the sampling locations.	24
Figure 11: Canonical analysis of principal coordinates (CAP) plots show differences for body morphometric of <i>Scomber colias</i> for the sampling locations.	25
Figure 12: Main structural areas of <i>S. colias</i> otolith (A–lateral face; B–medial face). Source: Figure produced by ICES, 2015.	25
Figure 13: Canonical variable plots show differences for the SI (A), EFD (B) and both SI + EFD (C), of the otolith of <i>Scomber colias</i> , respectively.	30
Figure 14: Canonical analysis of principal coordinates (CAP) plots for SI, EFD and both (SI + EFD) of the otolith of <i>Scomber colias</i> , respectively.	31

Figure 15: Elemental concentrations (mean \pm SE) in <i>Scomber colias</i> whole otoliths of two-year-old juvenile fish collected in Madeira, Canaries, Azores, Matosinhos, Sesimbra and Portimão. Ratios are given in μg element / g Ca. The locations marked with the same letter above the error bars are not significantly different concerning the elemental concentrations (Tukey test, $p>0.05$).	33
Figure 16: Isotopic signatures (mean \pm SE) in <i>S. colias</i> whole otoliths of two-year-old juvenile fish collected in Madeira, Canaries, Azores, Matosinhos, Sesimbra and Portimão. Ratios are given in ‰ VPDB. The locations marked with the same letter above the error bars are not significantly different concerning the isotopic signatures ($p>0.05$).	33
Figure 17: Canonical variable plot show differences for the elemental (A), isotopic (B) and both elemental + isotopic (C) of the otolith of <i>Scomber colias</i> , respectively.	36
Figure 18: Canonical analysis of principal coordinates (CAP) plots for isotopic (A), elemental (B), and both elemental + isotopic (C), of the otolith of <i>Scomber colias</i> , respectively.....	37

Índex of Tables

Table 1: Sampling location, sample size (N), fish total length (TL), fish weighed (W), of <i>Scomber colias</i> used to otolith shape analysis and body morphometric. Values are presented as mean \pm SE.....	11
Table 2: Sampling location, sample size (N), fish total length (TL), fish weighed (W) of <i>Scomber colias</i> used to otolith chemistry analysis. Values are presented as mean \pm SE.	11
Table 3: Anatomical landmarks defined along the body contour of <i>Scomber colias</i> used to determine the distances (from Erguden et al., 2009).	13
Table 4: Distances used to body morphometric analysis.....	14
Table 5: Formulas used to obtain otolith Shape Indices (SI) from the size parameters otolith length (OL, mm), otolith width (OW, mm), otolith area (OA, mm ²) and otolith perimeter (OP, mm) (from Tuset et al., 2003).....	17
Table 6: Tukey post-hoc test for distances morphometric (mm) of <i>Scomber colias</i> for the sampling locations. Values are presented as mean \pm SE.....	22

Table 7: Jackknifed classification matrix of the complete discriminant analysis for body morphometric of <i>Scomber colias</i> for the sampling locations.	23
Table 8: Tukey post-hoc test for otolith Shape Indices (SI) for the sampling locations. Values are presented as mean \pm SE.....	26
Table 9: Tukey post-hoc test for Elliptical Fourier Descriptors (EFD) for the sampling locations. Values are presented as mean \pm SE.....	26
Table 10: Jackknifed classification matrix of the complete discriminant analysis for otolith Shape Indices (SI) of <i>S. colias</i> for the sampling locations.	27
Table 11: Jackknifed re-classification matrix of the complete discriminant analysis for Elliptical Fourier Descriptors (EFD) of <i>Scomber colias</i> for the sampling locations.	28
Table 12: Jackknifed re-classification matrix of the complete discriminant analysis for otolith Shape Indices (SI) and Elliptical Fourier Descriptors (EFD) of <i>Scomber colias</i> for the sampling locations.	29
Table 13: Jackknifed re-classification matrix of the quadratic discriminant analysis for elemental signatures of the otolith of <i>Scomber colias</i> for the sampling locations.	34
Table 14: Jackknifed re-classification matrix of the quadratic discriminant analysis for isotopic signatures of the otolith of <i>Scomber colias</i> for the sampling locations.....	35
Table 15: Jackknifed re-classification matrix of the quadratic discriminant analysis for elemental e isotopic signatures of the otolith of <i>Scomber colias</i> for the sampling locations.	35

Abbreviations

ANOVA: One-way analysis of variance

ANCOVA: One-way analysis of covariance

CAP: Canonical analysis of principal coordinates

EFD: Elliptic Fourier descriptors

FAAS: Atomic absorption spectrometer

ICP-MS: Inductively coupled plasma mass spectrometry

LDFA: Linear discriminant function analyses

MANOVA: Multivariate analyses of variance

OA: Otolith area

OL: Otolith length

OP: Otolith perimeter

OW: Otolith weighed

QDFA: Quadratic discriminant function analyses

SB: Solution based

SI: Shape indices

SL: Standard length

TL: Fish total length

W: Fish weighed

1. INTRODUCTION

The Atlantic chub mackerel, *Scomber colias*, is one of the main pelagic fisheries resources in the Northeast Atlantic. *S. colias* is a fast growing early maturing species (Hernández and Ortega, 2000), usually found at depths between 250 to 300 m in warm and temperate waters of the Atlantic Ocean and in the Mediterranean Sea (Collette and Nauen, 1983; Collette, 1986).

In the Northeast Atlantic, *S. colias* is a species commercially exploited along the Iberian and North Africa coasts, but also in the Mediterranean Sea (Velasco et al., 2011). In recent years the commercial landing in the Iberian Peninsula has increased significantly in part as result of this species being the target for purse seiner fleets in Portugal and Spain (Villamor et al., 2017). The landings in Portugal in 2017 were 19477.8 t (DGRM, 2018).

Despite the increase of the catches, the information regarding the population structure, movement patterns and habitat connectivity of this species is, at present, still limited. However, some regional studies have recently been carried out on reproductive biology, age, growth, feeding habits and life history traits in the Azores (Carvalho et al., 2002), Canaries (Castro, 1993; Nespereira and Pajuelo, 1993; Lorenzo et al. 1995; Nespereira and Pajuelo 1996), Madeira (Silva, 1993; Vasconcelos, 2006; Vasconcelos et al., 2011; Vasconcelos et al., 2012), and Portugal mainland (Martins 1996; Martins and Cardador, 1996; Martins, 2007; Martins et al., 2013). These studies were important because despite the absence of physical barriers, marine fish species may show regional differences that could reveal the population structure scenario (Knutsen et al., 2003).

Some authors consider *S. colias* as single stock in the Northeast Atlantic based on mtDNA analysis (Scoles et al., 1998; Zardoya et al., 2004). For the appropriate management of exploited marine fish species it is important to know how the spatial distribution of fishing is related to populations structure, otherwise it is difficult to assess how fishing practices in one region could impact fisheries in others (Correia et al., 2011a). *S. colias* populations are not assessed in European waters (ICES, 2015), but scientific advice on this population may be required in the near future (Navarro et al., 2014). The limitation of data on the population dynamics of *S. colias* off Northeast Atlantic waters, prevent a better understanding of the ecosystem functioning and demands a more rational management of the fishing for this species (Martins et al., 2013).

1.1 Ecology

Originally *Scomber japonicus* (Houttuyn, 1782) was considered the species found in the Atlantic, Indian and Pacific Oceans (Collette and Nauen, 1983). But high levels of genetic divergence in nuclear and mitochondrial DNA have been reported (Scoles et al., 1998; Infante et al., 2007; Catanese et al., 2010), in which Indo-Pacific fish have remained *Scomber japonicus* and those fish of the Atlantic Ocean and related seas have been designated as *Scomber colias* (*Scomber colias* Gmelin, 1789).

However, *S. colias* is a commercially and ecologically important fish species, where the systematic state could be controversial due to the existence of geographically distant populations with morphological variability and wide distribution pattern, encompassing the North, South, West and East Atlantic, as well as the Mediterranean Sea (Collette and Nauen 1983).

S. colias has some typical morphological characteristics as a silvery white ventral and bluish to green dorsal with the presence of spots or wavy dashed lines (Figure 1). The pectoral fins are short and have 19 or 21 rays, the first dorsal fin originates behind the bases of the pectoral fin and has 9 or 10 spines and the second dorsal fin has 11 or 12 rays followed by five finlets. The space between the first and second dorsal fins is approximately equal to the length of the first dorsal fin (Collette and Nauen, 1983; Collette, 1986).



Figure 1: A *S. colias* specimen (23,4 cm of total length) collected in Portimão in February 2018 (personal photograph).

The larval fish growth is slow and almost in a linear way over the first 10 to 15 days and, subsequently they have a relatively high metabolic rate. The first feeding occurs 46 hours after hatching and all larvae have fed after 60 hours. Metamorphosis takes place

after 24 hours at 16.8°C or 16 days at 22.1°C (Castro-Hernández and Santana-Ortega, 2000).

In the spawning season adults migrate from the deeper cold waters of the upper slope and off the continental shelf to warm, temperate waters near the coast where temperature and available food, namely phytoplankton and microzooplankton, are more attractive to survival and development of the larvae (Hunter and Kimbell, 1980).

S. colias exhibits temporal sexual maturation differences throughout the Atlantic Ocean (Vasconcelos et al., 2012). The spawning season of the *S. colias* varies between regions, usually extending over a period of 3 to 5 months (Carvalho et al., 2002; Allaya et al., 2013). The spawning season in the Azores extends from March to August (Carvalho et al., 2002), from November to February in Canaries (Nespereira and Pajuelo, 1993), along the Portuguese coast fish spawn during February/March till May/June (Martins, 1996; Castro-Hernández and Santana-Ortega, 2000), and in the Madeira spawning occurs from January to May (Vasconcelos et al., 2012). This latitudinal gradient could be related to seawater temperature as the main spawning season of *S. colias* occurs when water temperature is at least 10°C and most often when it is 15 to 20°C (Collette e Nauen, 1983; Castro-Hernández and Santana-Ortega, 2000).

In the European Atlantic waters, spawning grounds and migrations are not well known (ICES, 2015). The lack of genetic differentiation across the northeast Atlantic and the Mediterranean Sea does not support the existence of homing behaviour to spawning grounds (Zardoya et al. 2004). Typically, pelagic fishes spawn in areas with high biological production to ensure the feeding of older larval states, with temperature playing a crucial role during spawning (Vasconcelos et al., 2012).

According to Nespereira and Pajuelo, (1996), in the Canaries, younger individuals are found in inshore coastal waters and when they reach a size close to 12 cm of total length they move to more distant areas off the coast, within the continental shelf, where they are captured by the fisheries fleets. When it reaches about 26 cm, individuals leave these areas, to go to the feeding areas located offshore. Every year, during the winter months, large adult individuals approach the coast for reproduction, returning to the offshore areas in late spring to feed.

In the Portuguese mainland waters *S. colias* reaches up to 20 cm total length in the first year of life and sexual maturity occurs at 1 - 2 years of age (Martins, 2007). In the Canaries the average size of the first spawn corresponds to approximately 20 cm of total length for both sexes, in which the first mature specimens are 16 cm in size

(Nespereira and Pajuelo, 1993). The males and females have the same life maturity pattern (Martins, 1996). The growth rate increases significantly during the second year of life, corresponding to a stage during which they migrate to deeper richer offshore waters, which appear to offer much better conditions for growth than coastal waters (Perrota et al., 2005). Hence, energy is probably driven to reproduction, resulting in less energy available for somatic growth (Nespereira and Pajuelo, 1993). According to Villamor et al. (2017), the age structure of *S. colias* in Atlantic Iberian waters is mainly composed by fish between 0-6 years old, with prevalence of ages 1 to 3.

This species presents a migratory pattern between costal and offshore areas, concerning spawning and also feeding behaviour (Castro-Hernández and Santana-Ortega, 2000). Both juveniles and adults feed mainly on zooplankton, although in adults feeding regime may range from copepods, invertebrates, crustaceans, squids, small pelagic fishes to fish eggs (Castro, 1993; Zardoya et al, 2004). This change in diet is related to older individuals tending to be more distributed offshore (Baird, 1978). In addition to the importance of *S. colias* as a fishery resource, it is also an important component for the diet of larger pelagic fish, sharks and marine mammals (Lockwood 1988; Zardoya et al., 2004).

Scoles et al. (1998) considered the existence of a single stock of *S. colias* in the Atlantic based on mtDNA analysis. Zardoya et al. (2004) affirms that there is an extensive gene flow between Mediterranean Sea and Atlantic Ocean populations of *S. colias*, which are organized into a larger panmictic unit, and the lack of structure found in *S. colias* in both sites is consistent with one stock management policy.

1.2 Spatial distribution and landings

In the Northeast Atlantic, *S. colias* is distributed from the southern part of the Atlantic European waters (Bay of Biscay and Iberian Peninsula), towards North West African coastal waters, including Canary Islands (Figure 2). It is also abundant in the Mediterranean and the southern part of the Black Sea (Whitehead et al, 1984).

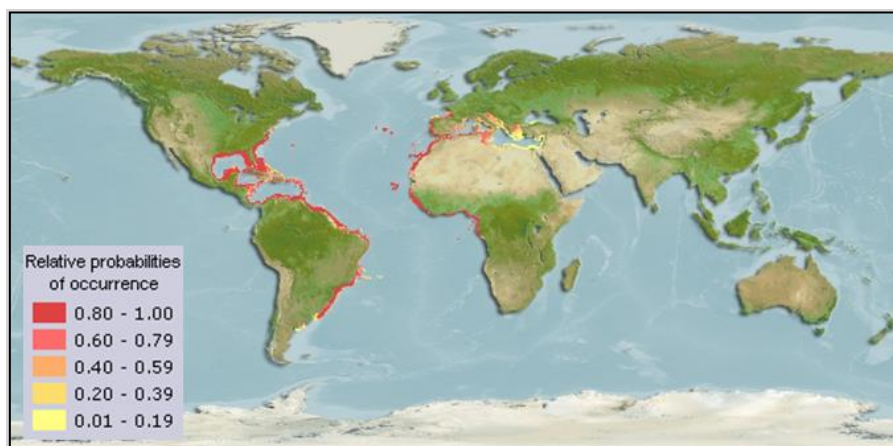


Figure 2: Distribution range colours indicate degree of suitability of habitat which can be interpreted as probabilities of occurrence of the *Scomber colias*. Source: Aquamaps. 2016. Reviewed Native Distribution Map for *Scomber colias* (Atlantic chub mackerel), with modelled year 2100 native range map based on IPCC A2 emissions scenario. www.aquamaps.org, version of Aug. 2016. Web. Accessed 4 Jun. 2018.

In the Northeast Atlantic the landings of *scomber colias* were 24,699 t in 2016 to 64199 t in 2016 (FAO, 2016). Since 2010 *S. colias* landings have notably increased on about 40% in relation to the previous periods. In Atlantic European waters, landings mainly come from the Spanish and Portuguese purse seiner fisheries, generally as a by-catch, but with a low market prize (Villamor et al., 2017).

The historical series of Spanish showed two different periods: before 2006, the catches remained at low level, and after this year, catches have continuously increasing until 2014, remaining then at more or less the same level (Villamor et al., 2017). In the Canaries, in 2006 catches were 475.86 t and increased to 634.84 t in 2009 (Gobierno de Canarias, 2018). This trend is similar to that observed in Portugal, since 1986, where Portuguese landings of *S. colias* ranged between 4000 and 23000 t, except the high level from the mid-1960s to the mid-1970s, and after fluctuated at a low level (ca. 10000 t per year) until the early 2000s and increased subsequently (Martins et al., 2013).

The total landing of *S. colias* in Portugal in 2017 was 19.477,8 t: 19.089,3 t from the mainland, 193,3 t from Azores and 195,2 t from Madeira. From the total landed on the Portugal mainland in 2017, 2.620,4 t were from Matosinhos, 10.839,8 t from Sesimbra, and 157,6 t from Portimão. The *S. colias* landed from Portugal mainland was 13.755,9 t by purse seine, 5.024,2 t by multi-purpose fishing, 309,1 t caught by trawling (DGRM, 2018).

Previously, *S. colias* was not a target species for the purse seiner fleets, being a by-catch mainly used as a bait for other fisheries (Correia, 2016). In Portugal, *S. colias*

is mainly caught in the purse seine fishery directed towards sardine. Recently, *S. colias* has grown in the total Portuguese purse-seine landings in part due to the fact that sardine abundance has decreased since 2006 (ICES, 2015).

This significant increase in catches can be explained by the decrease in sardine landings together with new market opportunities, especially as supply for the canning industry, as well as a possible increase of *S. colias* availability (Correia, 2016; Villamor et al., 2017). *S. colias* and *Sardina pilchardus* may affect each other through predation since both species consume fish egg, larvae and early juveniles; *S. colias* adults feed mainly of small pelagic species such as sardine and anchovy (Castro and Hernández-García, 1995).

Catches are mainly concentrated in the western part, where younger fish are predominant, while in the Cantabrian Sea the bulk of the catches are taken in the second half of the year, being mainly adult fish, although the amount of younger fish has increased in this area in the most recent years (Villamor et al., 2017).

1.3 Natural tags

The use of natural tags (e.g. body morphometrics, otolith shape and otolith fingerprinting), has been considered an efficient tool for fish stock identification (Stransky et al., 2008; Kaouèche et al., 2017; Moreira et al., 2018).

Geometric morphometrics is frequently employed to delineate fish stocks, and are continuous characteristics describing aspects of body shape (Erguden et al., 2009). Variation in such characteristics is due to both environmental and genetic components (Cabral et al., 2003). Regional morphometric data variation is useful to discriminate fish stock structure of various exploited marine fish species (Cabral et al., 2003; Erguden et al., 2009; Allaya et al., 2016), and can provide additional knowledge to a better management and conservation of fisheries (Dwivedi and Dubey, 2012).

The truss network protocol was described for character selection, which enforces systematic coverage of the shape and archives the landmark configuration (Strauss and Bookstein, 1982). According to Strauss and Bookstein (1982), the geometric protocol overcomes the disadvantages of traditional data sets (characters aligned along 1 axis, i.e., the longitudinal; coverage of forms that are highly uneven by region; repeated use of some morphological landmarks, etc) and systematically detect shape differences in oblique as well as horizontal and vertical directions. This is because it uses a system of

measures that ensures generally even coverage of the landmark configuration. The protocol archives the configuration of landmarks so that the form may be reconstructed from the set of distances among landmarks. Also recognize and compensate for random measurement error, and average the forms of a sample of individuals. Besides this, succinctly characterize and visualize multivariate trends of growth and allometry within populations and standardize forms for intergroup comparison (Strauss and Bookstein, 1982).

In addition to body morphometrics, the sclerochronology proprieties of otoliths are particularly useful to link environmental patterns to ontogenetic events experienced by individual fish (ICES, 2015).

Otoliths are paired calcified structures made of calcium carbonate (CaCO_3), mainly in the mineral form of aragonite, located in the inner ear of teleost fishes used for water balance and/or hearing (Poper et al., 2005). It begins to form before hatching and grow continuously through the life cycle preserving a record of fish environment (Campana 1999). Therefore, otoliths are considered as unique natural tags because grow continuously throughout life, remain chemically inert and preserve an uninterrupted record of the environment where fish lived (Campana, 1999). There are three pairs of otoliths located in the inner ear of teleost fishes, called *sagittae*, *lapilli* and *asterisci*, which vary considerably in format and size according to different species and ontogenetic stages (Volpedo and Vaz-dos-Santos, 2015). The *sagittae* are most often used otoliths because they are the largest, earliest formed and easiest to extract (Green et al., 2009). The first use of the otoliths in fisheries biology was the age estimates through annual, seasonal and daily increments. However, at present, otoliths are also widely used to study the environmental biology of fish and to delineate fish stocks (Volpedo and Vaz-dos-Santos, 2015).

Therefore, the otolith shape is also considered an efficient tool for fish stock identification (Campana and Neilson 1985; Ferguson et al., 2011; Jemaa et al., 2015) and has proven successful in resolving fish stock structure in high gene flow systems, when environmental heterogeneity exists (Bacha et al., 2014). Otolith shape is markedly species specific, but also shows intra-specific geographic variation in relation to environmental factors and fish growth (Ferguson et al., 2011; Jemaa et al., 2015).

The extent to which otolith shape differences are genetically or environmentally induced is still unclear, but sex, age, year classes, stock and environment should be take into consideration (Cardinale et al., 2004). While environment essentially alters the otolith

growth rate, which in turn modifies otolith shape, genetically induced changes can locally affect otolith shape (Cardinale et al., 2004).

However, the micro-chemical composition analysis has added another dimension to otolith studies (Green et al., 2009). Biogeochemical signatures encoded within otoliths are natural tags that are continuously recording information throughout the lifetime of a fish and can be used to infer differences in a range of ecological characteristics of a species such as differentiate among fish stocks (Thorrold et al., 1997).

If different fish populations inhabit different aquatic environments, or at least have a very prolonged exposure to different water environments, the otolith elemental composition should serve as a natural tag for these groups (Campana 1999). Moreover, oxygen and carbon stable isotope ratios have been also used successfully as natural tags for fish population structure studies (Gao et al., 2004; Correia et al., 2011a).

Thus, elemental or isotopic signatures of whole otoliths provide an environmental natural tag integrated over the fish's entire life, i.e. from birth until death (Campana et al., 2000).

2. OBJECTIVES

2.1 General Objective

The overall aim of this work was to assess the use of the shape and chemical signatures of otoliths and body morphometrics as an alternative approach to obtain new information about the population structure, fish movement and habitat connectivity of the chub mackerel (*Scomber colias*) in the NE Atlantic. This new information will be available to the decision-makers and fisheries agencies to promote a rational and sustainable management of this fishery.

2.2 Specific Objectives

Specifically, we intent to: i) examine the variation in otolith elemental and isotopic signatures for the whole otoliths (entire life-history prior to capture) in *S. colias* captured from different regions of the NE Atlantic to investigate whether these can be used to assess the degree of separation between stocks; ii) assess the use of otolith shape to

provide information on the population structure of *S. colias* from the NE Atlantic to determine whether may represent discrete populations; and iii) analyse the use of body morphometric as an alternative tool to obtain new information about the stock structure of *S. colias* from the different fishing grounds of the NE Atlantic.

3. MATERIALS AND METHODS

3.1 Samples collection

Fish samples were collected in Azores, Canaries, Madeira and Portugal mainland - Portimão, Sesimbra and Matosinhos (Figure 3), from January to April 2018. Juveniles (20 to 27 cm) were caught by purse seine and transported to the laboratory in isothermal containers with ice (Figure 4). The fish were measured (TL, 0.1 cm), weighed (W, 0.1 g) and photographed with the landmarks for the body morphometric analyses (Erguden et al., 2009). Thereafter both sagittal otoliths were extracted with plastic forceps to avoid metallic contamination, cleaned of organic tissues using distilled water, air dried and stored in Eppendorf vials until further analysis (age estimate, otolith shape and otolith chemistry analyses. Otoliths were differentiated to left and right sagittal according to position of the sulcus acusticus and the rostrum (Secor et al., 1992). The right otoliths were used to otolith shape and them to isotopic analysis and the left were used to elemental analysis.

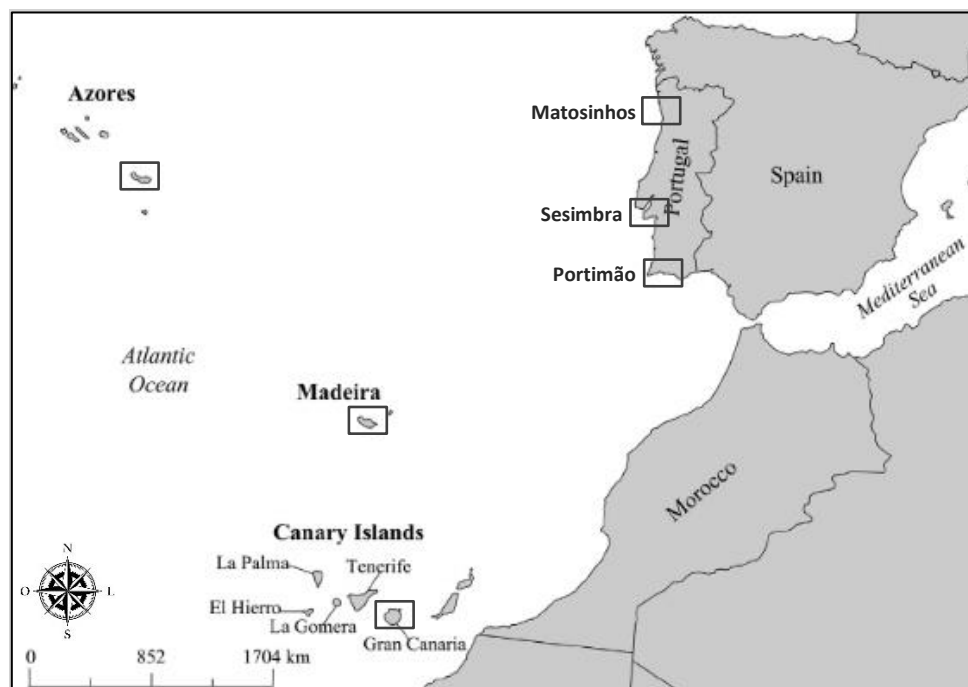


Figure 3: Sampling locations of *Scomber colias* caught in the NE Atlantic from January to April 2018.



Figure 4: *S. colias* collected in Matosinhos in the January 2018 (personal photograph).

A total of 270 samples (45 per location) were used for otolith shape analysis and body morphometric analysis (Table 1). Other 180 (30 per location) were used for otolith chemistry from individuals (Table 2) of age group 2 years.

Table 1: Sampling location, sample size (N), fish total length (TL), fish weighed (W), of *Scomber colias* used to otolith shape analysis and body morphometric. Values are presented as mean \pm SE.

REGION	SITES	N	TL (cm)	W (g)
Madeira	-	45	22.3 \pm 0.1	87.1 \pm 1.8
Canaries	-	45	22.3 \pm 0.2	84.7 \pm 1.9
Azores	-	45	24.1 \pm 0.2	128.4 \pm 3.8
Portugal Mainland	Matosinhos	45	23.5 \pm 0.2	98.8 \pm 4.2
	Sesimbra	45	21.5 \pm 0.2	67.0 \pm 1.7
	Portimão	45	23.2 \pm 0.2	93.7 \pm 2.2

Table 2: Sampling location, sample size (N), fish total length (TL), fish weighed (W) of *Scomber colias* used to otolith chemistry analysis. Values are presented as mean \pm SE.

REGION	SITES	N	TL (cm)	W (g)
Madeira	-	30	22.6 \pm 0.1	91.0 \pm 1.3
Canaries	-	30	22.5 \pm 0.1	88.1 \pm 1.8
Azores	-	30	23.9 \pm 0.2	127.4 \pm 4.1
Portugal Mainland	Matosinhos	30	23.1 \pm 0.1	90.8 \pm 2.5
	Sesimbra	30	21.8 \pm 0.2	69.8 \pm 1.8
	Portimão	30	23.1 \pm 0.1	91.0 \pm 1.6

3.1.1 Age estimates

Scomber colias otoliths have clear growth annual increments, where two bands, one opaque and one translucent, were laid down each year on the otoliths (Nespereira and Pajuelo, 1993). The opaque zone was mainly formed during the spring and summer months, when the temperature of the sea is higher, and the food is more abundant, and

the translucent one was formed during the autumn and winter months, when the spawning of this species occurs (Lorenzo, 1992). Under reflected light the increment opaque formed during periods of fast growth have a white appearance, while those translucent formed during the periods of slow growth have a dark appearance (Kiparissis et al., 2000).

The otoliths were immersed in a clearing agent (ethanol and glycerol, 1:1) to enhance their transparency during reading, with the distal surface turned up and the proximal surface (sulcus acusticus) turned down, and were examined using a stereomicroscope (Meiji Techno EMZ-13TR) against a dark background. Therefore, the age of each fish was assigned by counting the annual growth increments on sagittal otoliths according to an already existent standard protocol (ICES, 2015).

Therefore, the readers did not know the length of the fish and the reading was started from the posterior area, followed by the edge next to the rostrum area. It was taken into account the frequent presence of checks or false increments during the first years, which can be identified following this pattern of width decrease (checks does not follow the pattern). Otoliths were discarded when in a bad state and when there is a succession of annuli, where the readers cannot be sure if they are true annuli or checks.

The adopted birth date was 1st January and the capture occurred in the first semester. Therefore, when a translucent ring was observed at the edge of the otolith, it was counted as an annulus. Readings were performed by a two-independent reader, were select the otoliths with 100% concordance. Individuals of age group 2 years were selected from each region for further analyses. The Figure 5 shows a pair of otoliths of *S. colias* captured in Sesimbra of two-year-old according to the opaque and translucent increment shown in the image.

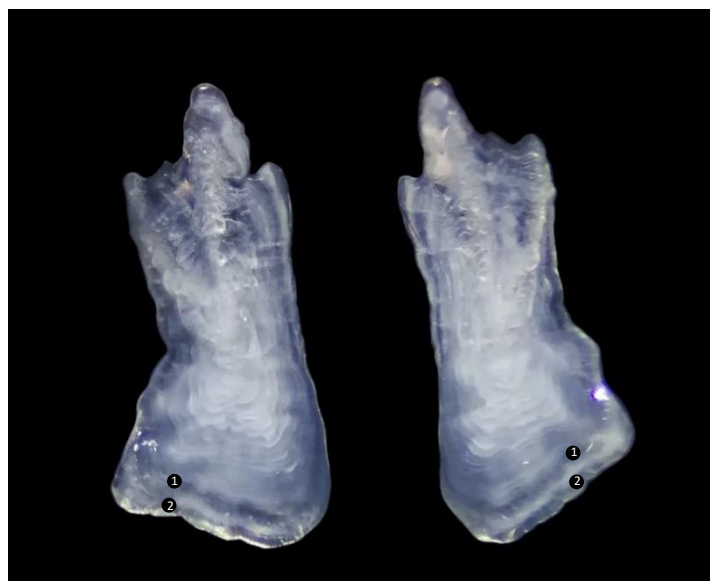


Figure 5: Otoliths of *Scomber colias* (23,1 cm of total length) collected in Sesimbra in 2018 (personal captation).

3.2 Body morphometric

For the analysis of the body morphometric the truss network system standard protocol described by Strauss and Bookstein (1982) was used. A total of 13 anatomical landmarks (Table 3) were defined along the body contour, determining 27 distances (Table 4), based on the morphometric study with this same species (Erguden et al., 2009).

Table 3: Anatomical landmarks defined along the body contour of *Scomber colias* used to determine the distances (from Erguden et al., 2009).

LANDMARKS	BODY LOCATION
1	Anterior tip of snout at upper jaw
2	Most posterior aspect of neurocranium (beginning of scaled nape)
3	Origin of dorsal fin
4	Insertion of dorsal fin
5	Origin of second dorsal fin
6	Insertion of second dorsal fin
7	Anterior attachment of dorsal membrane from caudal fin
8	Posterior end of vertebrae column

9	Anterior attachment of ventral membrane from caudal fin
10	Insertion of anal fin
11	Origin of anal fin
12	Insertion of pelvic fin
13	Posterior most point of maxillary

Table 4: Distances used to body morphometric analysis.

DISTANCES	LANDMARKS	DISTANCES	LANDMARKS	DISTANCES	LANDMARKS
1	1 to 2	10	3 to 12	19	6 to 10
2	1 to 12	11	3 to 10	20	7 to 8
3	1 to 13	12	4 to 5	21	7 to 9
4	2 to 3	13	4 to 10	22	7 to 10
5	2 to 11	14	4 to 11	23	8 to 9
6	2 to 12	15	5 to 6	24	9 to 10
7	2 to 13	16	5 to 10	25	10 to 11
8	3 to 4	17	6 to 7	26	11 to 12
9	3 to 11	18	6 to 9	27	12 to 13

The Figure 6 illustrated the truss network with the location of the landmarks determined for distances morphometric.

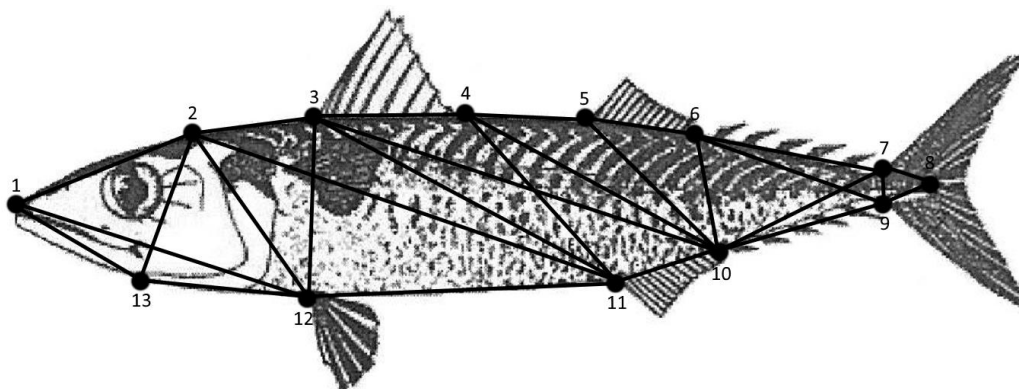


Figure 6: Locations of the 13 selected landmarks on the fish left side (adapted from Collette, 1986).

The left side of each fish, with the fins in the extended position, was photographed from a fixed distance with a high quality digital camera (Figure 7). Only undamaged fish

were included in the analyses. Landmarks were performed on digital images using TPSUTIL and TPSDIG. The user-friendly interface of the software allows the practitioner to precisely mark and record the X–Y coordinates of the positions of each landmark to build the truss network. Vertices were estimated from X and Y coordinates of all specimens according to the least square method (Rohlf and Slice, 1990).



Figure 7: *Scomber colias* collected from Azores in February 2018 (26,8 cm of total length) showing the body landmarks (personal photograph).

3.2.1 Statistical Analysis

For the Analysis of Covariance (ANCOVA), standard length (SL), instead of TL, was used as covariate, where is represented by the distance of the landmark 1 to 8. So, ANCOVA between morphometric distances and standard length of samples showed significant correlation. Location was treated as a fixed factor, and SL as covariate. So, the first step of the analyses was the allometric transformation given by Reist (1985) where size-dependent variation of morphometric characters was corrected to eliminate any variation resulting from allometric growth. Thus, the following transformation was used: $D = \log M - \beta (\log SL - \log MSL)$, where M is the original morphometric measurement, D is the transformed morphometric measurement, β is the slope of the regression of log M on Log SL, SL is the standard length of fish, MSL is the overall mean of standard length for all fish from all samples for each variable.

Body geometric morphometrics were investigated by uni and multivariate statistical analyses. One-way analysis of variance (ANOVA) was performed to assess the significant differences of each morphometric distances between the six regions, followed by a Tukey post-hoc test if significant ($p < 0.05$), used to determine significantly different subsets. Multivariate analyses were performed with a complete quadratic discriminant function analyses (QDFA). Jackknifed classification matrix was used to calculate the percentage of correctly reclassified specimens into original sample and to discriminate between the six sites. A canonical analysis of principal coordinates (CAP) based on Euclidian distances was performed to identify the vectors of the components and their respective contributions. All statistical analyses were performed using the software Systat v.12 and PRIMER 6+PERMANOVA.

3.3 Otolith shape analysis

The right otolith was recorded using reflected light against a dark and homogenous background obtained using a stereomicroscope (Meiji Techno EMZ-13TR) coupled with a USB digital camera (Olympus, SC30). Otoliths were positioned with the sulcus acusticus up, with the rostrum pointed to the left. Care has been taken to avoid that the curvature of the otolith produces any deviation or error in the results (Volpedo and Vaz-dos-Santos, 2015). The B&W contrasts to binary digital images (Figure 8) were obtained using the free software Paintnet, and thereafter the images were processed using the free softwares ImageJ (SI - Shape Indices) and Shape Analysis v. 1.3 (EFD - Elliptic Fourier Descriptors).

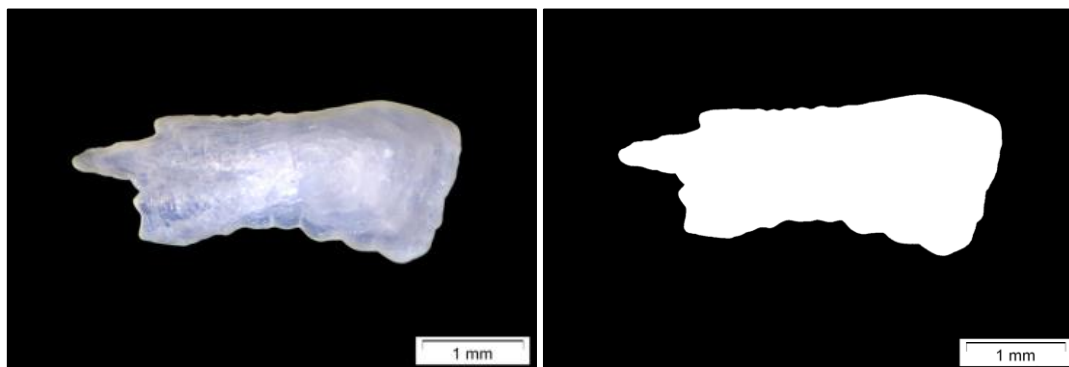


Figure 8: Right otolith sagittal photograph of the *Scomber colias* and the corresponding binary digital image, respectively.

Using the software ImageJ size parameters such as otolith length (OL, mm), otolith width (OW, mm), otolith area (OA, mm²) and otolith perimeter (OP, mm) were obtained. With this data it was possible to calculate five shape indices (SI) (Table 5) as form factor (FF), roundness (RO), ellipticity (EL), circularity (CI) and rectangularity (RE), according to Tuset et al. (2003).

Table 5: Formulas used to obtain otolith Shape Indices (SI) from the size parameters otolith length (OL, mm), otolith width (OW, mm), otolith area (OA, mm²) and otolith perimeter (OP, mm) (from Tuset et al., 2003).

Shape Indices (SI)	Formulas
Form factor (FF)	$(4\pi OA)/OP^2$
Roundness (RO)	$(4OA)/(\pi OL^2)$
Circularity (CI)	OP^2/OA
Rectangularity (RE)	$OA/(OL \times OW)$
Ellipticity (EL)	$(OL - OW)/(OL + OW)$

The program Shape v.1.3 was used to extract the contour otolith shape (Figure 9) and to determine the number of elliptic Fourier descriptors (EFD) required to adequately describe the otolith outline (Ferguson et al., 2011). The first 6 harmonics reached >95% of the cumulative power indicating (excluding coefficient d_6), that the otolith shape could summarize by 23 Fourier coefficients, i.e. $6 \times 4 - 1 = 23$. In the shape program, the elliptical Fourier harmonics for each otolith were normalized to the first harmonic and were thus invariant to otolith size (Kuhl and Giardina, 1982), so the first three coefficients (a_1 , b_1 and c_1) constant for all outlines has been excluded, reducing the number of EFD to 20.

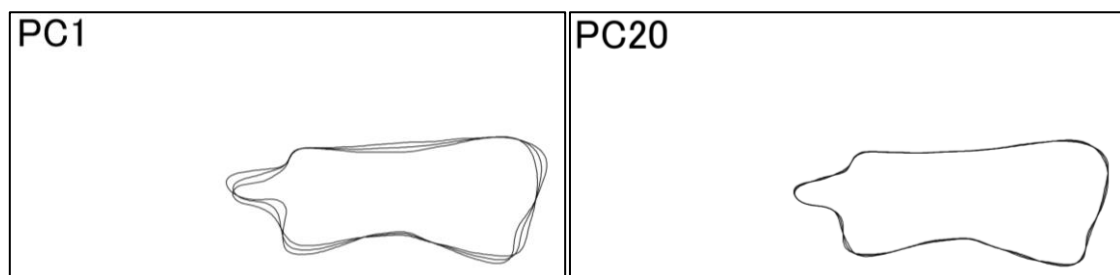


Figure 9: Contour otolith shape of 1 Principal component (23% significance cumulative) of 20 Principal components (95% significance cumulative) (Output EFD).

3.3.1 Statistical Analysis

The data were checked for normality (Shapiro–Wilk test, $P > 0.05$) and homogeneity of variances (Levene's test, $P > 0.05$). All assumptions were satisfied after log 10 transformation (CI). Relationships between SI and OL (as covariate) were tested with analysis of covariance (ANCOVA). Location was treated as fixed factor. EL and CI showed positive relationship with OL ($r^2 = 0.0624$, $n = 270$, $p < 0.05$; $r^2 = 0.0708$, $n = 270$, $p < 0.05$, respectively). FF, RO and RE concentrations showed negative relationship with OL ($r^2 = 0.0812$, $n = 270$, $p < 0.05$; $r^2 = 0.1403$, $n = 270$, $p < 0.05$; $r^2 = 0.0624$, $n = 270$, $p < 0.05$, respectively). All variables have been corrected using the ANCOVA slope. The formula used to correct it was $V_{adj} = V - (\beta \times OL)$, where V_{adj} is the transformed value, V is the original value, β is the slope of the ANCOVA of SI on OL and OL is the otolith length (Campana and Casselman 1993; Cardinale et al. 2004; Ferguson et al. 2011). One-way analysis of variance (ANOVA) was used to explore the differences in SI and EFD between locations, followed by a Tukey post-hoc if needed ($p < 0.05$). EFD and SI were analysed with a complete linear discriminant function analysis (LDFA) to examine the percentage of correctly reclassified individuals from jack-knife (leave-one-out cross-validation) procedures. Canonical analysis of principal coordinates (CAP) based on Euclidian distances was used to observe the separation between groups and the vectors of the components that most contribute to this discrimination.

All statistical analyses were using the software Systat v.12 and PRIMER 6+PERMANOVA.

3.4 Otolith Chemistry Analysis

Elemental and isotopic signatures of whole otolith were determined by inductively coupled plasma mass spectrometry (ICP-MS-SB) and isotope ratio mass spectrometry (IRMS), respectively.

Prior to chemical analyses, otolith's pair was rinsed in ethanol and brushed in Milli-Q water to remove any glycerol contamination (Campana, 1999). The glycerol would take 1 to 2 months of immersion to enter otoliths (Campana et al., 2003).

Thereafter otoliths were decontaminated in an ultrasonic bath for 5 min in ultrapure water (Milli-Q water) to remove any adherent biological tissues, followed by immersion

in 3% analytical grade hydrogen peroxide (H_2O_2) for 15 min to remove any remaining biological residues (Rooker et al., 2001).

3.4.1 Elemental Signatures

The left whole otoliths were immersed in ultrapure 1% nitric acid (HNO_3) solution for 10 s to remove superficial contamination, followed by a double-immersion in Milli-Q water during 5 min to remove the acid (Rooker et al., 2001). Then otoliths were stored in decontaminated Eppendorf tubes (acid leached/rinsed), where the otoliths were allowed to air dry in a laminar flow cabine hood (Patterson et al. 1999; Rooker et al. 2001; Daros et al. 2016). The decontaminated left otoliths were weighed on an analytical balance (0.000001 g), dissolved for 15 min in 60 μ l of ultrapure HNO_3 and diluted with Milli-Q water to a final volume of 3 ml (2% of HNO_3 v/v and 0.02% of TDS m/v). The solution was stirred with a vortex and was sent to analysis.

Multi-elemental analysis was performed by ICP-MS using an iCAPTM Q (Thermo Fisher Scientific, Bremen, Germany) instrument equipped with a concentric glass nebulizer, a Peltier-cooled baffled cyclonic spray chamber, a standard quartz torch and a two-cone interface design (sample and skimmer cones). High-purity (99.9997%) argon (Gasin II, Leça da Palmeira, Portugal) was used as the nebulizer and plasma gas. The equipment control and data acquisition were made through the Qtegra software (Thermo Fisher Scientific, Bremen, Germany). The ICP-MS was operated under the following conditions: RF power, 1550W; argon flow rate, 14 L/min; auxiliary argon flow rate, 0.8 L/min; nebulizer flow rate, 0.98 L/min. Indium (^{115}In) was monitored as internal standard. Only the ^{44}Ca was analysed by FAAS - Flame Atomic Absorption Spectrometry instrument (Perkin Elmer, Überlingen, Germany).

Otolith samples were analysed in random order to avoid possible sequence effects. For quality control, precision and accuracy checks, the NRC otolith certified reference material FEBS-1 was analysed (Sturgeon et al., 2005). Elemental concentrations determined in FEBS-1 were within the certified or indicative range, with a value of recovery >95%. The precision of replicate analyses of individual elements ranged between 2% and 5% of the relative standard deviation (RSD).

Thirteen elements: ^{44}Ca (0.015 mg/L), ^{23}Na (0.403 μ g/L), ^{88}Sr (0.079 μ g/L), 7Li (0.002 μ g/L), ^{26}Mg (0.044 μ g/L), ^{52}Cr (0.051 μ g/L), ^{55}Mn (0.019 μ g/L), ^{59}Co (0.006 μ g/L), ^{60}Ni (0.009 μ g/L), ^{65}Cu (0.022 μ g/L), ^{75}As (0.119 μ g/L), ^{85}Rb (0.024 μ g/L) and ^{137}Ba (0.007 μ g/L) were detectable in otoliths of *S. colias*. ^{44}Ca provided the internal standard. Data

were also collected for ^9Be (0.004 $\mu\text{g/L}$), ^{66}Zn (0.252 $\mu\text{g/L}$), ^{82}Se (0.354 $\mu\text{g/L}$), ^{95}Mo (0.006 $\mu\text{g/L}$), ^{111}Cd (0.003 $\mu\text{g/L}$), ^{118}Sn (0.005 $\mu\text{g/L}$), ^{121}Sb (0.002 $\mu\text{g/L}$), ^{205}Tl (0.002 $\mu\text{g/L}$), ^{209}Pb (0.001 $\mu\text{g/L}$) and ^{238}U (0.0004 $\mu\text{g/L}$), but their concentrations were below the limit of detection. The trace elements concentrations, originally in $\mu\text{g element L}^{-1}$ solution, were transformed to $\mu\text{g element volume}^{-1}$ solution and then to $\mu\text{g element g}^{-1}$ otolith and finally to $\mu\text{g element g}^{-1}$ calcium.

3.4.2 Isotopic Signatures

Stable isotope ratios, namely $\delta^{13}\text{C}$ and $\delta^{18}\text{O}$, measured by standard mass spectrometric techniques in whole otolith samples. The right otoliths were triple-rinsed with Milli-QWater, air-dried in a laminar flow cabinet (Patterson et al., 1999) and weighed (0.000001 g). Otoliths were individually crushed into a fine carbonate powder using a previously decontaminated (using acetone) ceramic mortar and pestle and with the help of a paint-brush were transferred in Eppendorf microcentrifuge of 1.5 ml. Otolith samples were analysed in random order to avoid possible sequence effects.

$\delta^{13}\text{C}$ and $\delta^{18}\text{O}$ isotopic ratios were measured using a Delta V Advantage mass spectrometer coupled to an automated system (GasBench II). About 0.6 - 0.7 μg of carbonate was used for each sample. Each sample, duly numbered, was placed in a glass vial (10 ml) which was then sealed with a rubber septum cap. Seventy bottles were processed in each round of analysis (run), using a multi-flow unit of which 16 bottles correspond to the 4 reference standards, 2 international (NBS-19 and NBS-18) and two, internal (REI and VICK). Initially, flasks went through the flush step (240 seconds), which consists of a He gas jet to remove atmospheric gases (CO_2 and H_2O). After the flush, 90 mg (equivalent to $\sim 50 \mu\text{l}$) of H_3PO_4 acid were automatically added into each sample to release CO_2 from the carbonate. After addition of H_3PO_4 , the samples were allowed to react for 90 minutes at 70°C before being analysed. The He- CO_2 mixture released from each sample is then automatically transferred to the Delta V Advantage gas source mass spectrometer, and then the C and O isotopic ratios are measured.

3.4.3 Statistical Analysis

Elemental concentrations ($\mu\text{g element g}^{-1}$ calcium) and isotopic concentration (‰ VPDB) were checked for normality (Shapiro–Wilk test, $P>0.05$) and homogeneity of

variances (Levene's test, $P > 0.05$) prior to statistics. To meet these assumptions Cr:Ca was performed on log10 transformed data.

The relationship between elemental/isotopic concentration and otolith mass was tested with analysis of covariance (ANCOVA) using otolith mass as a covariate. Location was treated as fixed factor. Relationships between isotopic ratios ($\delta^{13}\text{C}$ and $\delta^{18}\text{O}$) and otolith mass (covariant) were not significant (ANCOVA, $p > 0.05$). ^{23}Na and ^{75}As concentrations showed positive relationship with otolith mass ($r^2 = 0.0346$, $n = 180$, $p < 0.05$; $r^2 = 0.0235$, $n = 180$, $p < 0.05$, respectively). ^7Li and ^{137}Ba concentrations showed negative relationship with otolith mass ($r^2 = 0.0219$, $n = 180$, $p < 0.05$; $r^2 = 0.0003$, $n = 180$, $p < 0.05$, respectively).

Since any fish size differences among samples could influence differences in whole otolith chemistry among regions, thereby potentially confounding the spatial variation in elemental chemistry, otolith elemental concentrations were corrected (Gerard and Muhling, 2010). The concentration of elements was weight-detrended by subtraction of the common within-group linear slope multiplied by the otolith mass from the observed concentration (Campana et al. 2000).

One-way analyses of variance (ANOVA) was used to detect regional differences in the concentrations, followed Tukey post-hoc test if needed ($p < 0.05$), to examine the existence of any significant differences in isotopic and elemental among the six sampling locations. Multivariate analyses of variance (MANOVA), was used to test for spatial differences in otolith multielemental and isotopic signatures. Quadratic discriminant function analyses (QDFA) were used to visualize spatial differences and to examine the re-classification accuracy of fishes to this original location, verified through percentage of correctly classification accuracies of the discriminant functions for each region using classification matrix Jackknife. The elemental and isotopic data was analyzed by a Canonical Analysis of principal Coordinates (CAP) based on Euclidian distances.

All statistical analyses were performed using software Systat v.12 and PRIMER 6 + PERMANOVA.

4. RESULTS

4.1 Body morphometrics

The One-way analysis of variance showed significant differences in 25 distances morphometric calculated (ANOVA, $p < 0.05$). The distances 17 and 18 showed no significant differences between locations (ANOVA, $p > 0.05$). Tukey post-hoc test, where shown the differences between the sampling locations (Table 6).

Table 6: Tukey post-hoc test for transformed morphometric measurement (D) of *Scomber colias* for the sampling locations. Values are presented as mean \pm SE. For each line (D), regions sharing the same letter does not show any statistical difference ($p > 0.05$).

D	Canaries	Azores	Madeira	Portimão	Matosinhos	Sesimbra
1	1.619 \pm 0.003 ^a	1.587 \pm 0.003 ^b	1.594 \pm 0.003 ^b	1.614 \pm 0.003 ^a	1.613 \pm 0.003 ^a	1.626 \pm 0.003 ^a
2	1.792 \pm 0.001 ^a	1.795 \pm 0.001 ^a	1.790 \pm 0.001 ^a	1.804 \pm 0.001 ^b	1.802 \pm 0.001 ^b	1.811 \pm 0.001 ^c
3	1.431 \pm 0.003 ^{a,b}	1.394 \pm 0.002 ^c	1.408 \pm 0.002 ^d	1.422 \pm 0.002 ^{a,e}	1.415 \pm 0.002 ^{d,e}	1.435 \pm 0.003 ^b
4	1.423 \pm 0.003 ^a	1.469 \pm 0.002 ^b	1.455 \pm 0.003 ^c	1.462 \pm 0.003 ^{b,c}	1.457 \pm 0.002 ^{b,c}	1.454 \pm 0.002 ^c
5	1.973 \pm 0.001 ^a	1.986 \pm 0.001 ^b	1.986 \pm 0.001 ^b	1.981 \pm 0.001 ^b	1.982 \pm 0.002 ^b	1.972 \pm 0.001 ^a
6	1.588 \pm 0.002 ^{a,b}	1.595 \pm 0.002 ^a	1.576 \pm 0.002 ^c	1.581 \pm 0.002 ^{b,c}	1.590 \pm 0.002 ^{a,d}	1.584 \pm 0.002 ^{b,c}
7	1.506 \pm 0.002 ^{a,d}	1.489 \pm 0.002 ^{b,c}	1.483 \pm 0.003 ^b	1.503 \pm 0.003 ^d	1.500 \pm 0.003 ^{c,d}	1.498 \pm 0.003 ^{c,d}
8	1.475 \pm 0.004 ^a	1.440 \pm 0.003 ^b	1.442 \pm 0.004 ^b	1.438 \pm 0.004 ^b	1.429 \pm 0.006 ^b	1.452 \pm 0.004 ^{a,b}
9	1.846 \pm 0.001 ^{a,b}	1.849 \pm 0.001 ^a	1.847 \pm 0.001 ^a	1.839 \pm 0.002 ^{b,c}	1.846 \pm 0.002 ^{a,c}	1.831 \pm 0.001 ^d
10	1.558 \pm 0.002 ^a	1.562 \pm 0.003 ^a	1.535 \pm 0.003 ^{b,c}	1.526 \pm 0.003 ^b	1.548 \pm 0.004 ^{a,c}	1.528 \pm 0.002 ^b
11	1.928 \pm 0.001 ^a	1.918 \pm 0.001 ^b	1.916 \pm 0.001 ^{b,c}	1.918 \pm 0.001 ^b	1.919 \pm 0.001 ^b	1.911 \pm 0.001 ^c
12	1.459 \pm 0.005 ^a	1.482 \pm 0.003 ^{a,b}	1.468 \pm 0.004 ^{a,b}	1.467 \pm 0.005 ^{a,b}	1.489 \pm 0.006 ^b	1.457 \pm 0.005 ^a
13	1.755 \pm 0.002 ^a	1.759 \pm 0.002 ^a	1.752 \pm 0.002 ^a	1.755 \pm 0.002 ^a	1.761 \pm 0.004 ^a	1.739 \pm 0.002 ^b
14	1.655 \pm 0.002 ^a	1.673 \pm 0.002 ^b	1.666 \pm 0.002 ^{a,b}	1.657 \pm 0.002 ^a	1.670 \pm 0.004 ^{a,b}	1.634 \pm 0.003 ^c
15	1.305 \pm 0.004 ^a	1.288 \pm 0.004 ^{a,b}	1.286 \pm 0.006 ^{a,b}	1.298 \pm 0.004 ^{a,b}	1.277 \pm 0.006 ^b	1.285 \pm 0.004 ^{a,b}
16	1.517 \pm 0.002 ^a	1.510 \pm 0.003 ^{a,b}	1.508 \pm 0.002 ^{a,b}	1.508 \pm 0.002 ^{a,b}	1.504 \pm 0.003 ^b	1.484 \pm 0.002 ^c
17	1.587 \pm 0.002 ^a	1.586 \pm 0.002 ^a	1.587 \pm 0.003 ^a	1.578 \pm 0.003 ^a	1.585 \pm 0.004 ^a	1.574 \pm 0.003 ^a
18	1.597 \pm 0.002 ^a	1.598 \pm 0.002 ^a	1.600 \pm 0.003 ^a	1.594 \pm 0.002 ^a	1.598 \pm 0.004 ^a	1.589 \pm 0.003 ^a
19	1.344 \pm 0.003 ^a	1.348 \pm 0.003 ^a	1.340 \pm 0.002 ^a	1.323 \pm 0.003 ^b	1.335 \pm 0.005 ^{a,b}	1.299 \pm 0.003 ^c

20	0.930±0.008 ^a	0.982±0.005 ^{b,c}	1.001±0.006 ^b	0.961±0.005 ^{a,c}	0.979±0.006 ^{b,c}	0.971±0.005 ^{b,c}
21	0.829±0.005 ^a	0.827±0.004 ^a	0.811±0.004 ^{a,c}	0.797±0.004 ^{b,c}	0.784±0.005 ^b	0.779±0.004 ^b
22	1.601±0.002 ^{a,c}	1.607±0.002 ^a	1.597±0.002 ^{a,c}	1.581±0.003 ^b	1.588±0.002 ^{b,c}	1.583±0.002 ^b
23	0.993±0.007 ^{a,b}	0.995±0.004 ^{a,b}	1.008±0.005 ^b	0.969±0.005 ^a	0.981±0.007 ^{a,b}	0.977±0.005 ^a
24	1.567±0.002 ^{a,b}	1.577±0.002 ^a	1.570±0.002 ^{a,c}	1.556±0.003 ^b	1.563±0.002 ^{b,c}	1.561±0.002 ^{b,c}
25	1.237±0.005 ^a	1.197±0.005 ^b	1.167±0.005 ^c	1.216±0.005 ^{a,b}	1.198±0.005 ^b	1.219±0.005 ^{a,b}
26	1.839±0.002 ^{a,c}	1.855±0.001 ^{b,d}	1.864±0.002 ^b	1.844±0.002 ^c	1.846±0.002 ^{c,d}	1.832±0.002 ^a
27	1.563±0.002 ^a	1.588±0.002 ^b	1.575±0.002 ^c	1.590±0.002 ^b	1.587±0.002 ^b	1.588±0.002 ^b

Jackknife reclassification accuracies showed a good overall reclassification success of 74% (Table 7). Samples from Canaries (91%) showed the best reclassification success. The misclassification was more common within the samples from the Matosinhos (47%).

Table 7: Jackknifed classification matrix of the complete discriminant analysis for body morphometric of *Scomber colias* for the sampling locations.

Original locations	Predicted locations						%CORRECT
	AZORES	CANARIES	MADEIRA	MATOSINHOS	PORTIMÃO	SESIMBRA	
AZORES	35	0	6	3	1	0	78
CANARIES	1	41	1	1	1	0	91
MADEIRA	6	0	35	2	2	0	78
MATOSINHOS	6	0	4	21	6	8	47
PORTIMÃO	1	1	1	5	32	5	71
SESIMBRA	1	0	0	6	2	36	80
TOTAL	50	42	47	38	44	49	74

Therefore, both QDFA plot was able to clearly isolate the Canaries from the other locations, (Figure 10). In addition, the samples that overlap most are from Portuguese coast (Matosinhos, Portimão and Sesimbra) and also between the Azores and Madeira. So, it is possible to observe three groups, Canaries (Group 1), Azores and Madeira (Group 2), and Matosinhos, Portimão and Sesimbra (Group 3).

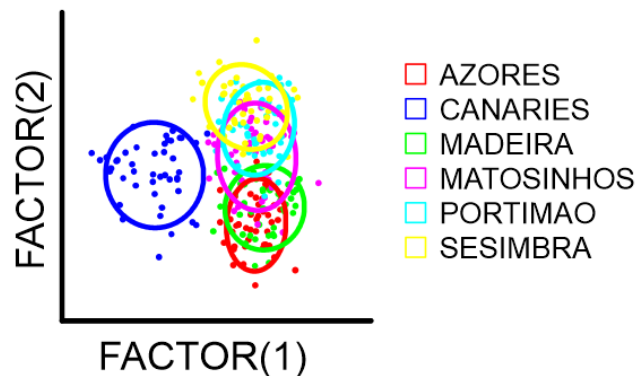


Figure 10: Canonical variable plots show differences for body morphometric of *Scomber colias* for the sampling locations.

The CAP showed the vectors of the components and their respective contributions to the discrimination of the sample locations (Figure 11). So, mainly the vectors for distances 8 (landmark 3 to 4) and 11 (landmark 3 to 10) were aligned with Group 1, the vectors for distances 9 (landmark 3 to 11), 14 (landmark 4 to 11), 19 (landmark 6 to 10), 22 (landmark 7 to 10) and 26 (landmark 11 to 12) were aligned with Groups 2, and the vectors for distances 1 (landmark 1 to 2), 2 (landmark 1 to 12) and 3 (landmark 1 to 13) were aligned with Groups 3. The distances 8 and 11 are biggest on the Group 1; the distances 9, 14, 19, 22, 26 and 19 are biggest on the Group 2; and the distances 1, 2 and 3 are biggest on the Group 3.

The distances 8 and 11 are more is more related to the length of the dorsal fin and distance from origin of dorsal fin to origin of anal fin, where in the Canaries it is bigger in both. The distances 9, 14, 19, 22, 26, 26 and 19 is more related to the height and length of the fish, where Azores and Madeira showed larger in these distances. The distances 1, 2 and 3 is clearly related to head length and mouth size, where Portugal mainland showed to be larger than in the islands.

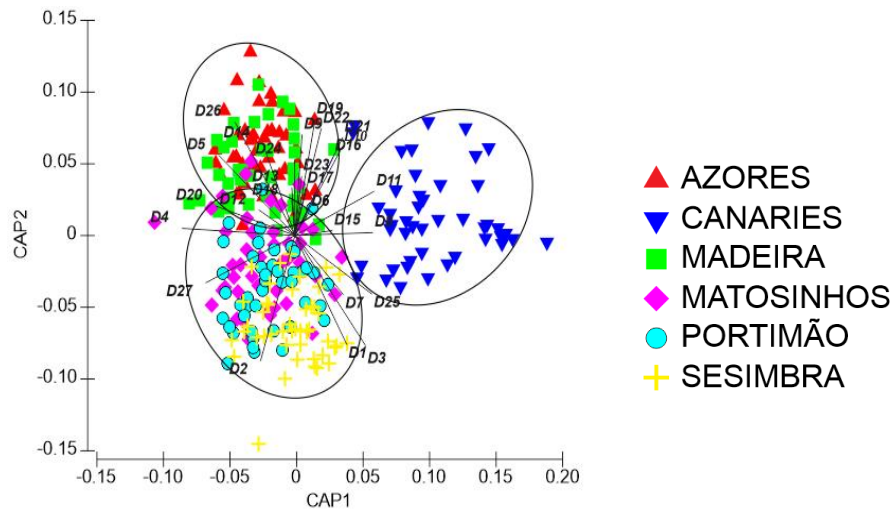


Figure 11: Canonical analysis of principal coordinates (CAP) plots show differences for body morphometric of *Scomber colias* for the sampling locations.

4.2 Otolith Shape

S. colias otoliths are thin have an irregular shape (Fig. 12) which is more accentuated in otoliths of older individuals (ICES, 2015).

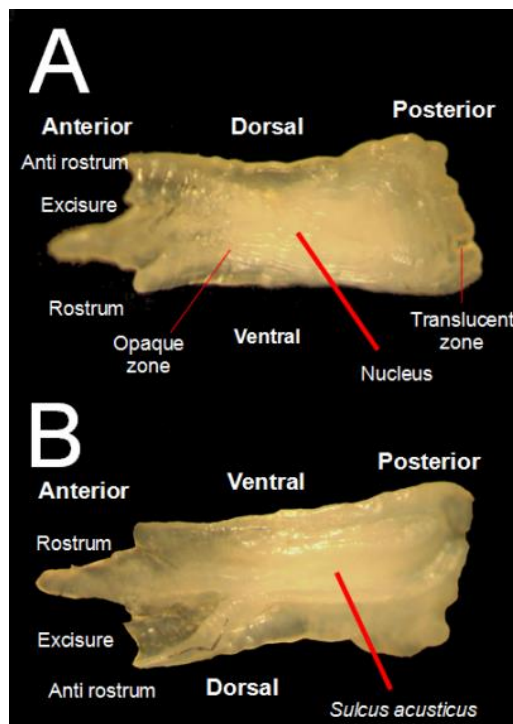


Figure 12: Main structural areas of *S. colias* otolith (A-lateral face; B-medial face). Source: Figure produced by ICES, 2015.

The One-way analysis of variance showed significant differences for the SI and EFD (ANOVA, $p < 0.05$). Tukey post-hoc test, where shown the differences between the sampling locations (Table 8 and 9). The RO, RE and EL, and EFDs showed differences between locations (ANOVA, $p < 0.05$). The shape indices FF and CI, and EFDs C2, B3, C4, D4 and A5 showed no significant differences between locations (ANOVA, $p > 0.05$).

Table 8: Tukey post-hoc test for otolith Shape Indices (SI) for the sampling locations. Values are presented as mean \pm SE. For each line (SI), regions sharing the same letter does not show any statistical difference ($p > 0.05$).

SI	Canaries	Azores	Madeira	Portimão	Matosinhos	Sesimbra
FF	0.524 \pm 0.003 ^a	0.520 \pm 0.003 ^a	0.536 \pm 0.003 ^a	0.532 \pm 0.003 ^a	0.521 \pm 0.004 ^a	0.526 \pm 0.003 ^a
RO	0.489 \pm 0.002 ^{a,b}	0.487 \pm 0.003 ^{a,c}	0.499 \pm 0.003 ^b	0.480 \pm 0.003 ^{a,c}	0.481 \pm 0.003 ^{a,c}	0.478 \pm 0.003 ^c
EL	0.335 \pm 0.002 ^{a,b}	0.331 \pm 0.003 ^a	0.330 \pm 0.003 ^a	0.340 \pm 0.003 ^{a,b}	0.337 \pm 0.003 ^{a,b}	0.343 \pm 0.004 ^b
CI	1.364 \pm 0.004 ^a	1.369 \pm 0.004 ^a	1.362 \pm 0.004 ^a	1.355 \pm 0.003 ^a	1.368 \pm 0.005 ^a	0.798 \pm 0.004 ^a
RE	0.807 \pm 0.003 ^{a,b}	0.796 \pm 0.003 ^a	0.819 \pm 0.004 ^b	0.796 \pm 0.003 ^a	0.794 \pm 0.003 ^a	0.418 \pm 0.003 ^a

Table 9: Tukey post-hoc test for Elliptical Fourier Descriptors (EFD) for the sampling locations. Values are presented as mean \pm SE. For each line (EFD), regions sharing the same letter does not show any statistical difference ($p > 0.05$).

SI	Canaries	Azores	Madeira	Portimão	Matosinhos	Sesimbra
D1	0.418 \pm 0.002 ^{a,b}	0.418 \pm 0.003 ^{a,b}	0.423 \pm 0.003 ^a	0.410 \pm 0.003 ^b	0.419 \pm 0.003 ^{a,b}	0.418 \pm 0.003 ^{a,b}
A2	0.024 \pm 0.002 ^a	0.0094 \pm 0.001 ^b	0.015 \pm 0.002 ^b	0.012 \pm 0.002 ^b	0.011 \pm 0.002 ^b	0.016 \pm 0.001 ^{a,b}
B2	0.030 \pm 0.001 ^a	0.019 \pm 0.003 ^b	0.027 \pm 0.001 ^{a,b}	0.030 \pm 0.001 ^a	0.024 \pm 0.002 ^{a,b}	0.028 \pm 0.002 ^a
C2	-0.006 \pm 0.002 ^a	-0.009 \pm 0.001 ^a	-0.013 \pm 0.002 ^a	-0.013 \pm 0.002 ^a	-0.010 \pm 0.003 ^a	-0.008 \pm 0.002 ^a
D2	0.065 \pm 0.001 ^a	0.064 \pm 0.001 ^a	0.059 \pm 0.001 ^b	0.058 \pm 0.001 ^b	0.056 \pm 0.001 ^b	0.055 \pm 0.001 ^b
A3	0.030 \pm 0.001 ^a	0.036 \pm 0.001 ^b	0.036 \pm 0.001 ^b	0.044 \pm 0.001 ^c	0.049 \pm 0.001 ^c	0.045 \pm 0.002 ^c
B3	0.001 \pm 0.001 ^a	0.005 \pm 0.001 ^a	0.004 \pm 0.001 ^a	0.0001 \pm 0.001 ^a	0.002 \pm 0.001 ^a	0.002 \pm 0.001 ^a
C3	-0.007 \pm 0.001 ^{a,b}	-0.005 \pm 0.001 ^a	-0.013 \pm 0.001 ^{b,c}	-0.016 \pm 0.002 ^c	-0.011 \pm 0.002 ^{a,b,c}	-0.011 \pm 0.002 ^{a,b,c}
D3	0.094 \pm 0.001 ^a	0.099 \pm 0.001 ^{a,b}	0.099 \pm 0.001 ^{b,c}	0.104 \pm 0.001 ^{c,d}	0.108 \pm 0.001 ^d	0.104 \pm 0.001 ^{c,d}
A4	-0.008 \pm 0.001 ^{a,b,c}	-0.010 \pm 0.001 ^{a,c}	-0.011 \pm 0.001 ^a	-0.008 \pm 0.001 ^{a,c}	-0.0064 \pm 0.0009 ^b	-0.004 \pm 0.001 ^b
B4	0.028 \pm 0.001 ^a	0.018 \pm 0.003 ^b	0.021 \pm 0.001 ^{a,b}	0.026 \pm 0.001 ^{a,b}	0.022 \pm 0.001 ^{a,b}	0.024 \pm 0.001 ^{a,b}
C4	0.0229 \pm 0.0009 ^a	0.020 \pm 0.003 ^a	0.024 \pm 0.001 ^a	0.0235 \pm 0.0009 ^a	0.025 \pm 0.001 ^a	0.023 \pm 0.001 ^a
D4	0.042 \pm 0.001 ^a	0.041 \pm 0.001 ^a	0.041 \pm 0.001 ^a	0.042 \pm 0.001 ^a	0.038 \pm 0.001 ^a	0.038 \pm 0.001 ^a
A5	0.004 \pm 0.001 ^a	0.0024 \pm 0.0008 ^a	0.003 \pm 0.001 ^a	0.0041 \pm 0.0009 ^a	0.0049 \pm 0.0008 ^a	0.004 \pm 0.001 ^a

B5	-0.006±0.001 ^{a,c}	0.001±0.001 ^b	-0.004±0.001 ^{a,b,d}	-0.009±0.001 ^c	-0.006±0.001 ^{c,d}	-0.008±0.001 ^{a,c,d}
C5	-0.0006±0.0007 ^{a,b}	0.0002±0.001 ^a	-0.003±0.001 ^{a,b}	-0.003±0.001 ^{a,b}	-0.0034±0.0007 ^b	-0.0038±0.0009 ^b
D5	-0.0182±0.0008 ^a	-0.0213±0.0006 ^b	-0.016±0.001 ^a	-0.0168±0.0006 ^a	-0.0160±0.0007 ^a	-0.0155±0.0008 ^a
A6	-0.028±0.001 ^{a,c}	-0.0253±0.001 ^{a,c}	-0.028±0.001 ^a	-0.027±0.001 ^{b,c}	-0.0210±0.0009 ^b	-0.019±0.001 ^b
B6	0.0260±0.0009 ^a	0.017±0.003 ^b	0.021±0.001 ^{a,b}	0.025±0.001 ^a	0.022±0.001 ^{a,b}	0.025±0.001 ^a
C6	-0.0066±0.0006 ^a	-0.0038±0.0008 ^{a,b}	-0.003±0.001 ^b	-0.0027±0.0008 ^b	-0.0009±0.0007 ^b	-0.0010±0.0006 ^b

Jackknife reclassification based on the SI, showed a very low overall reclassification success of 27% meaning that was a great misclassification of individuals to the original location. Samples from Madeira were allocated to all the sampled locations, but with more individuals being assigned to originals locations than other locations. All other sampled locations have been assigned to different locations than the originals (Table 10). However, the best classification percentage was obtained for Madeira (51%) with some individuals being allocated mainly in the Canaries. The second-best classification percentage was obtained for Portimão (44%).

The misclassification was more common within the samples from the Matosinhos (9%), Sesimbra (18%) and Canaries (18%). Individuals from Matosinhos presented higher allocation in Portimão, individuals from Sesimbra presented higher allocation in Portimão and individuals from Canaries resented higher allocation in Madeira. There was a misallocation among individuals of all sites, with a higher but more subtle allocation between Azores, Canaries and Madeira, and between Matosinhos, Portimão and Sesimbra.

Table 10: Jackknifed classification matrix of the complete discriminant analysis for otolith Shape Indices (SI) of *S. colias* for the sampling locations.

Original location	Predicted locations						%CORRECT
	AZORES	CANARIES	MADEIRA	MATOSINHOS	PORTIMÃO	SESIMBRA	
AZORES	11	8	7	10	8	1	24
CANARIES	8	8	15	3	9	2	18
MADEIRA	5	8	23	3	1	5	51
MATOSINHOS	10	7	8	4	14	2	9
PORTIMÃO	7	5	2	5	20	6	44
SESIMBRA	8	6	3	2	18	8	18

TOTAL	49	42	58	27	70	24	27
--------------	----	----	----	----	----	----	-----------

Using the EFD, the allocation of samples improved the overall reclassification to a success of 50% (Table 11). Samples from Canaries, Azores and Madeira being more frequently assigned original locations. All other sampled locations have been assigned to different locations than the originals. However, the best classification percentage was obtained for Canaries (76%) with some individual allocated mainly in the Azores and Madeira. The second-best classification percentage was obtained for Azores (58%) with some individuals allocated mainly in the Canaries and Madeira.

The misclassification was more common within the samples from the Sesimbra (31%) and Portimão (36%), where the samples from Sesimbra was more frequently allocation for Matosinhos and samples from Portimão some individuals were allocated mainly in the Sesimbra. Therefore, it was observed that the individuals of the islands had higher allocation among them (Azores, Canaries and Madeira) and the individuals of mainland Portugal had greater allocation among them (Matosinhos, Portimão and Sesimbra), where only a few individuals are allocated between the two groups (islands and mainland Portugal).

Table 11: Jackknifed re-classification matrix of the complete discriminant analysis for Elliptical Fourier Descriptors (EFD) of *Scomber colias* for the sampling locations.

Original locations	Predicted locations						%CORRECT
	AZORES	CANARIES	MADEIRA	MATOSINHOS	PORTIMÃO	SESIMBRA	
AZORES	26	9	6	3	1	0	58
CANARIES	5	34	3	1	1	1	76
MADEIRA	3	6	24	4	7	1	53
MATOSINHOS	1	0	3	21	9	11	47
PORTIMÃO	2	2	6	8	16	11	36
SESIMBRA	2	0	2	15	12	14	31
TOTAL	39	51	44	52	46	38	50

Using the combination of both shape descriptors (SI and EFD), the re-allocation of samples to the original location slightly improved the overall reclassification success to 51% (Table 12). The best classification rate was obtained for the Canaries (73%),

followed by Matosinhos (58%) and Azores (53%). Some individuals from the Canaries were misclassified mainly in the Madeira and Azores. Some individuals from the Matosinhos were misclassified mainly in the Sesimbra and Portimão, and some individuals from the Azores were misclassified mainly in the Canaries and Madeira.

The lowest reclassification success was obtained for Sesimbra (29%). The samples from Sesimbra were more frequently misclassified in the Matosinhos followed by Portimão. However, as noted for EFD, occurred the allocation of individuals mostly within two groups (oceanic islands and Portugal mainland), and possibly this occurred due mainly to the EFD.

Table 12: Jackknifed re-classification matrix of the complete discriminant analysis for otolith Shape Indices (SI) and Elliptical Fourier Descriptors (EFD) of *Scomber colias* for the sampling locations.

Original locations	Predicted locations						%CORRECT
	AZORES	CANARIES	MADEIRA	MATOSINHOS	PORTIMÃO	SESIMBRA	
AZORES	24	8	8	2	2	1	53
CANARIES	4	33	5	0	2	1	73
MADEIRA	7	10	23	2	2	1	51
MATOSINHOS	0	0	1	26	7	11	58
PORTIMÃO	0	3	5	5	20	12	44
SESIMBRA	2	0	2	15	13	13	29
TOTAL	37	54	44	50	46	39	51

Therefore, the LDFA plot (Figure 13) showed a high overlap of individuals from all sampling locations for the SI, for the EFD and for both combined. A slightly better separation between the sample locations occurred with SI and EFD combined. When SI and EFD were used alone, perception is more difficult, especially for SI that are highly overlapping. It is possible to observe a high degree of overlap of individuals from all sampling locations. In addition to the high overlap, it is possible to observe two groups, where there is bigger overlap between individuals from the Canaries, Azores and Madeira (Group 1) and from Matosinhos, Portimão and Sesimbra (Group 2).

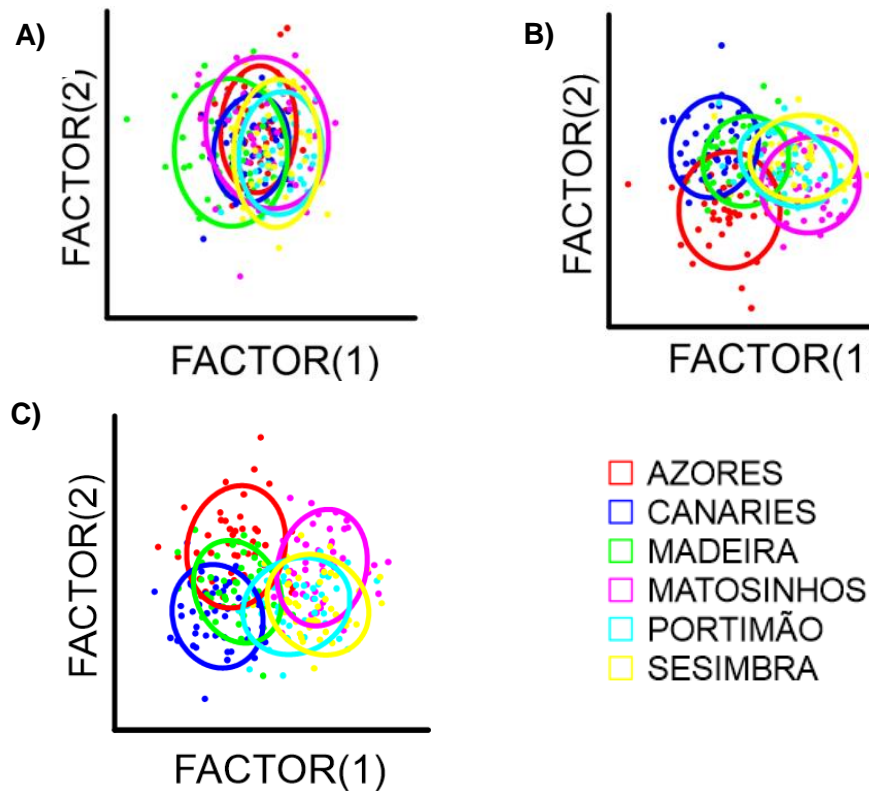
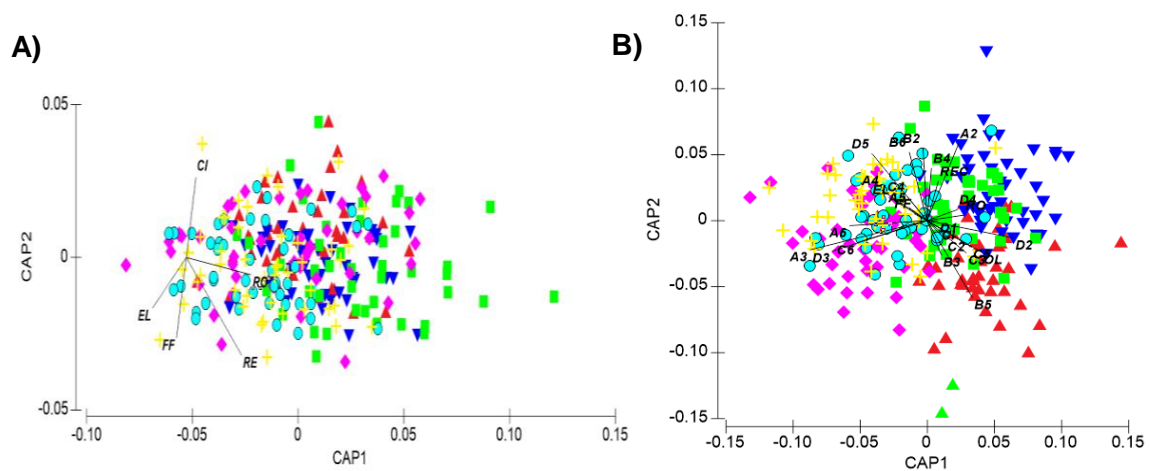


Figure 13: Canonical variable plots show differences for the SI (A), EFD (B) and both SI + EFD (C), of the otolith of *Scomber colias*, respectively.

The Canonical analysis of principal coordinates (CAP) showed the vectors of the components and their respective contributions to the discrimination of the sample locations (Figure 14). The vectors for RE, RO, A2, B5 and D2 were aligned with Group 1 and the vectors for EL, A3, D3 and D5 were aligned with Groups 2.



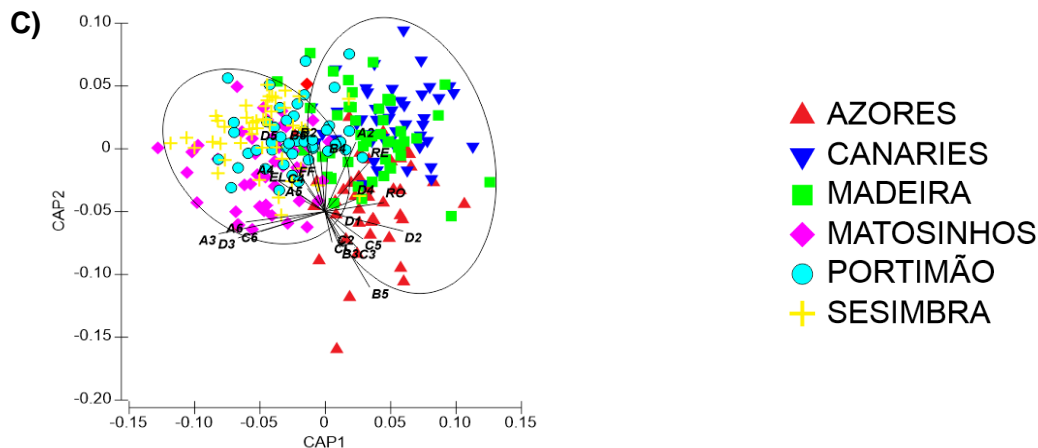
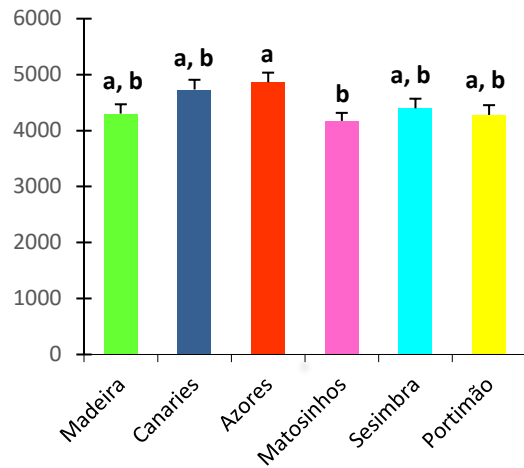


Figure 14: Canonical analysis of principal coordinates (CAP) plots for SI, EFD and both (SI + EFD) of the otolith of *Scomber colias*, respectively.

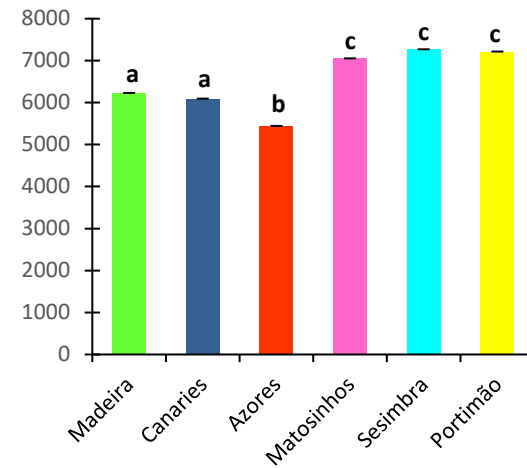
4.3 Otolith Chemistry

The otolith elemental chemistry recorded significant differences for Na:Ca, Sr:Ca, Li:Ca, Mg:Ca, Rb:Ca, Ba:Ca and Mn:Ca (ANOVA, $p < 0.05$). However Cr:Ca, Ni:Ca, Cu:Ca, As:Ca and Co:Ca were no significant different among locations (ANOVA, $p > 0.05$). The Tukey post-hoc test (Figure 15) about the Na:Ca showed significant differences only between Matosinhos and Azores; about the Sr:Ca no significant differences between Canaries and Madeira, between Portugal mainland (Matosinhos, Portimão and Sesimbra); about the Li:Ca, no significant differences between Azores and Madeira and between Portugal mainland (Matosinhos, Sesimbra and Portimão); about the Mg:Ca significant differences between Canaries and all others samples locations; about the Mn:Ca no significant differences between Azores and Madeira, between Azores and Canaries, between Madeira, Matosinhos and Sesimbra and between Portugal mainland (Matosinhos, Sesimbra and Portimão); about the Rb:Ca significant differences between Azores and all others samples locations and between Canaries and Matosinhos; and finally about the Ba:Ca significant differences only between Canaries and all others sample locations.

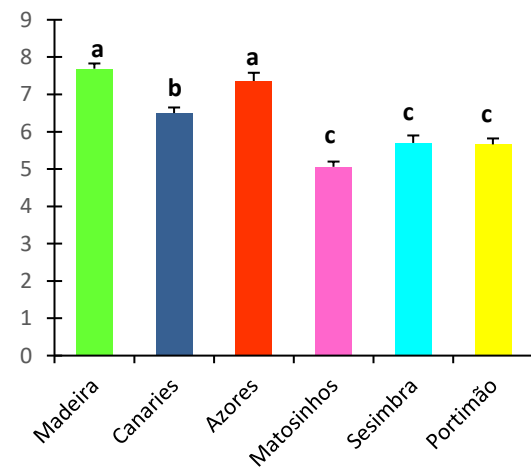
Na:Ca



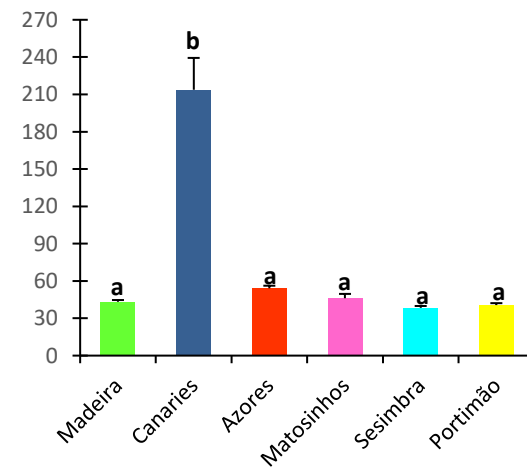
Sr:Ca



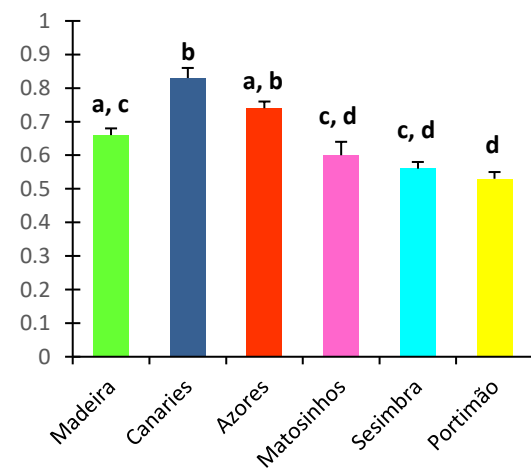
Li:Ca



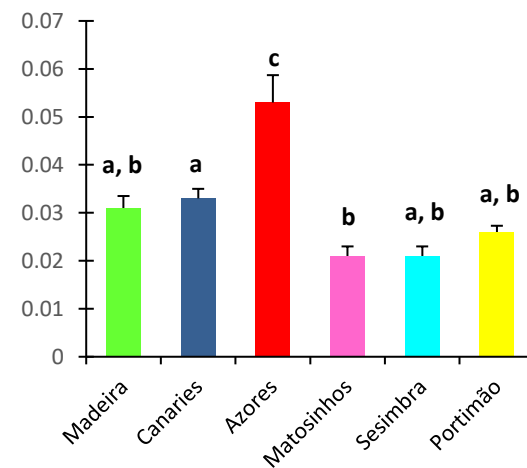
Mg:Ca



Mn:Ca



Rb:Ca



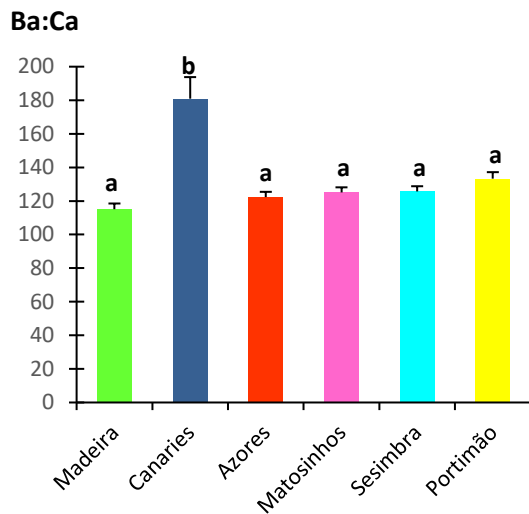


Figure 15: Elemental concentrations (mean ± SE) in *Scomber colias* whole otoliths of two-year-old juvenile fish collected in Madeira, Canaries, Azores, Matosinhos, Sesimbra and Portimão. Ratios are given in µg element / g Ca. The locations marked with the same letter above the error bars are not significantly different concerning the elemental concentrations (Tukey test, $p > 0.05$).

The overall otolith isotopic ratios ranged from -5.82‰ to 1.71‰ for $\delta^{13}\text{C}$ and from -8.19‰ to -0.99‰ for $\delta^{18}\text{O}$. The otolith isotopic chemistry recorded significant differences values of $\delta^{13}\text{C}$ and $\delta^{18}\text{O}$ among locations (ANOVA, $p < 0.05$). The Tukey post-hoc test showed no significant differences between Canaries and Madeira and between Matosinhos and Portimão for $\delta^{13}\text{C}$ (Tukey tests, $p > 0.05$), and no significant differences between Azores, Canaries and Madeira and between Portimão and Sesimbra for $\delta^{18}\text{O}$ (Tukey tests, $p > 0.05$) (Figure 16).

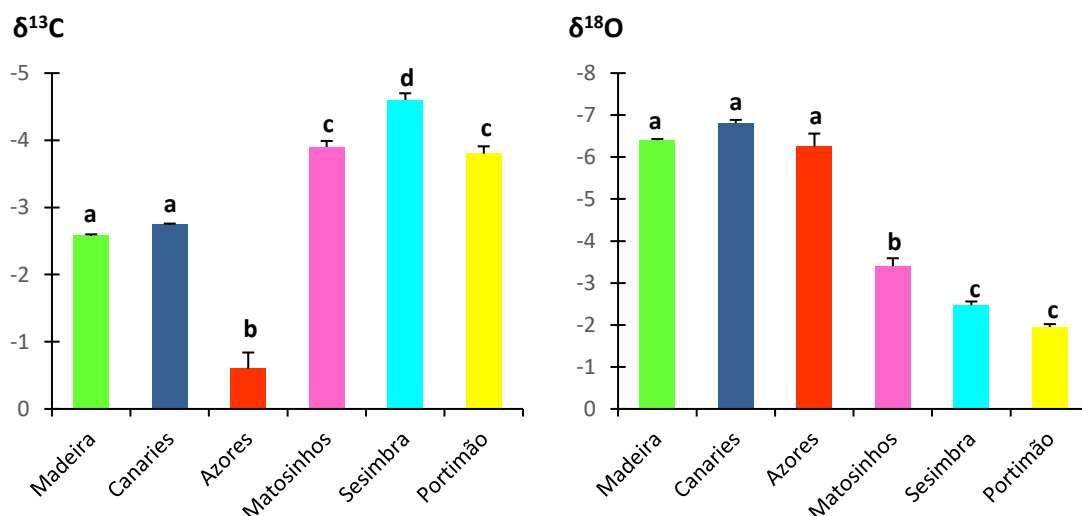


Figure 16: Isotopic signatures (mean ± SE) in *S. colias* whole otoliths of two-year-old juvenile fish collected in Madeira, Canaries, Azores, Matosinhos, Sesimbra and Portimão. Ratios are given in ‰ VPDB. The locations marked with the same letter above the error bars are not significantly different concerning the isotopic signatures ($p > 0.05$).

Jackknife reclassification accuracies based on the otolith elemental ratios were moderate to high for the islands and low to moderate to Portugal mainland (Table 13). Reclassification showed a moderate overall reclassification success of 59%. Samples from the islands Canaries (97%), Azores (73%), and Madeira (60%) showed a best reclassification success while the Sesimbra (33%) and Portimão (34%) showed a low reclassification success and Matosinhos (57%) a moderate reclassification success.

Samples from Canaries and Azores (best reclassification) were not allocated to any location of the mainland Portugal and the samples from the three sites of the Portugal mainland allocated mainly between them, i.e. there was a higher allocation between Azores, Canaries and Madeira, and between Matosinhos, Portimão and Sesimbra.

Table 13: Jackknifed re-classification matrix of the quadratic discriminant analysis for elemental signatures of the otolith of *Scomber colias* for the sampling locations.

Original locations	Predicted locations						%CORRECT
	AZORES	CANARIES	MADEIRA	MATOSINHOS	PORTIMÃO	SESIMBRA	
AZORES	22	1	7	0	0	0	73
CANARIES	1	29	0	0	0	0	97
MADEIRA	3	2	18	0	2	5	60
MATOSINHOS	0	0	0	17	4	9	57
PORTIMÃO	0	1	3	6	10	9	34
SESIMBRA	0	0	4	8	8	10	33
TOTAL	26	33	32	31	24	33	59

Regarding the isotopic ratios, the QDFA showed a better reallocated success than elemental, with 81% (Table 14). The Azores was the best classification percentage with 100% of the samples assigned to the original location. The seconds best classification percentage was obtained for Canaries and Madeira (87%) with some individuals allocated between them. The misclassification was more common within the samples from the Matosinhos (63%), where some samples was allocation to Portimão and Sesimbra. As occurred in the elemental QDFA, but now clearer, the misclassification was mainly between Portugal mainland (Matosinhos, Portimão and Sesimbra).

Table 14: Jackknifed re-classification matrix of the quadratic discriminant analysis for isotopic signatures of the otolith of *Scomber colias* for the sampling locations.

Original locations	Predicted locations						%CORRECT
	AZORES	CANARIES	MADEIRA	MATOSINHOS	PORTIMÃO	SESIMBRA	
AZORES	30	0	0	0	0	0	100
CANARIES	0	26	4	0	0	0	87
MADEIRA	0	4	26	0	0	0	87
MATOSINHOS	2	0	0	19	3	6	63
PORTIMÃO	0	0	0	1	23	6	77
SESIMBRA	0	0	0	2	7	21	70
TOTAL	32	30	30	22	33	33	81

Using the combination of both elemental and isotopic (Table 15), jackknife reclassification accuracies was high for the islands Azores (100%), Canaries (100%) and Madeira (90%), and was moderate for the Portugal mainland (Matosinhos, Portimão and Sesimbra). The samples from the island (Canaries, Azores and Madeira) were not allocated to mainland (Matosinhos, Portimão and Sesimbra) and the opposite also occurs.

Table 15: Jackknifed re-classification matrix of the quadratic discriminant analysis for elemental e isotopic signatures of the otolith of *Scomber colias* for the sampling locations.

Original locations	Predicted locations						%CORRECT
	AZORES	CANARIES	MADEIRA	MATOSINHOS	PORTIMÃO	SESIMBRA	
AZORES	30	0	0	0	0	0	100
CANARIES	0	30	0	0	0	0	100
MADEIRA	1	2	27	0	0	0	90
MATOSINHOS	0	0	0	21	2	7	70
PORTIMÃO	0	0	0	8	13	8	45
SESIMBRA	0	0	0	5	7	18	60
TOTAL	31	32	27	34	22	33	78

The QDFA plot (Figure 17) showed that elemental and isotopic ratios combined discriminates better the individuals presenting a clear separation between locations. Also

showed on elemental the bigger distinction of the Canaries, Madeira/Azores and Matosinhos/Portimão/Sesimbra. In the plot of the isotopic it is clearer the distinction of the Azores, Madeira/Canaries and Matosinhos/Portimão/Sesimbra. For the both elemental and isotopic, the separation of the four main groups becomes clearer, with distinction between Canaries (Group 1), Azores (Group 2), Madeira (Group 3) and Portugal mainland (Group 4).

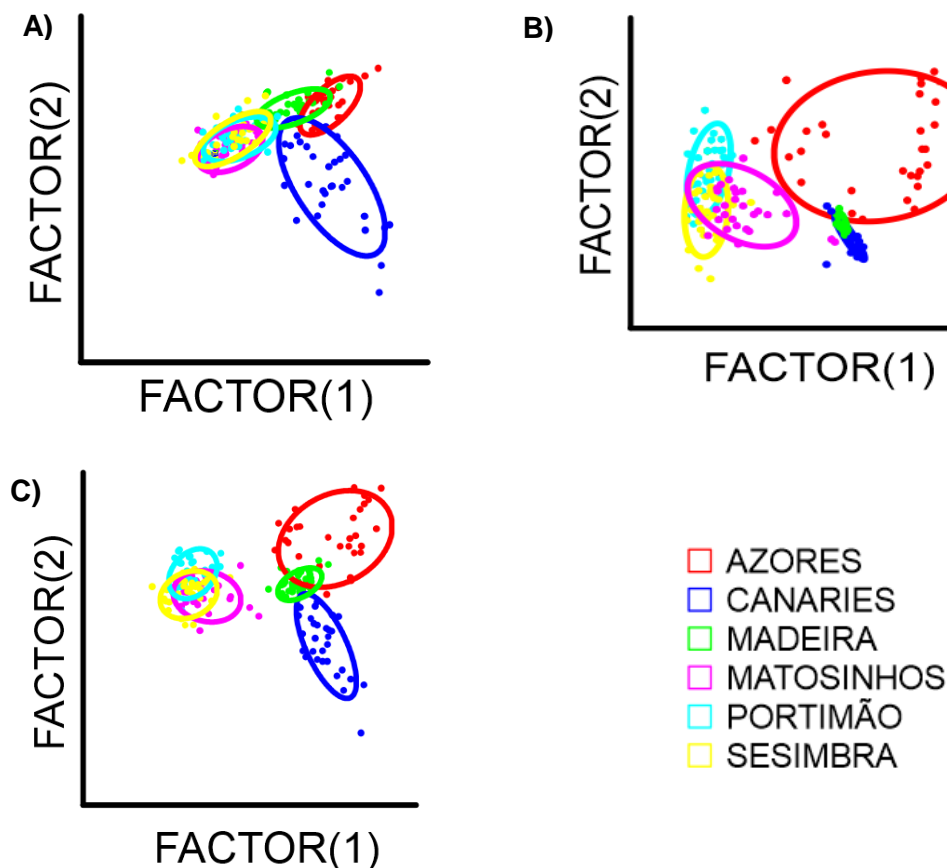


Figure 17: Canonical variable plot show differences for the elemental (A), isotopic (B) and both elemental + isotopic (C) of the otolith of *Scomber colias*, respectively.

The Canonical analysis of principal coordinates (CAP) showed that mainly the vectors for Mg:Ca, Ba:Ca were aligned with Group 1; Rb:Ca, $\delta^{13}\text{C}$ were aligned with Group 2; Mn:Ca and Li:Ca were aligned with Group 3; and Sr:Ca and $\delta^{18}\text{O}$ were aligned with Group 4 (Figure 18, C).

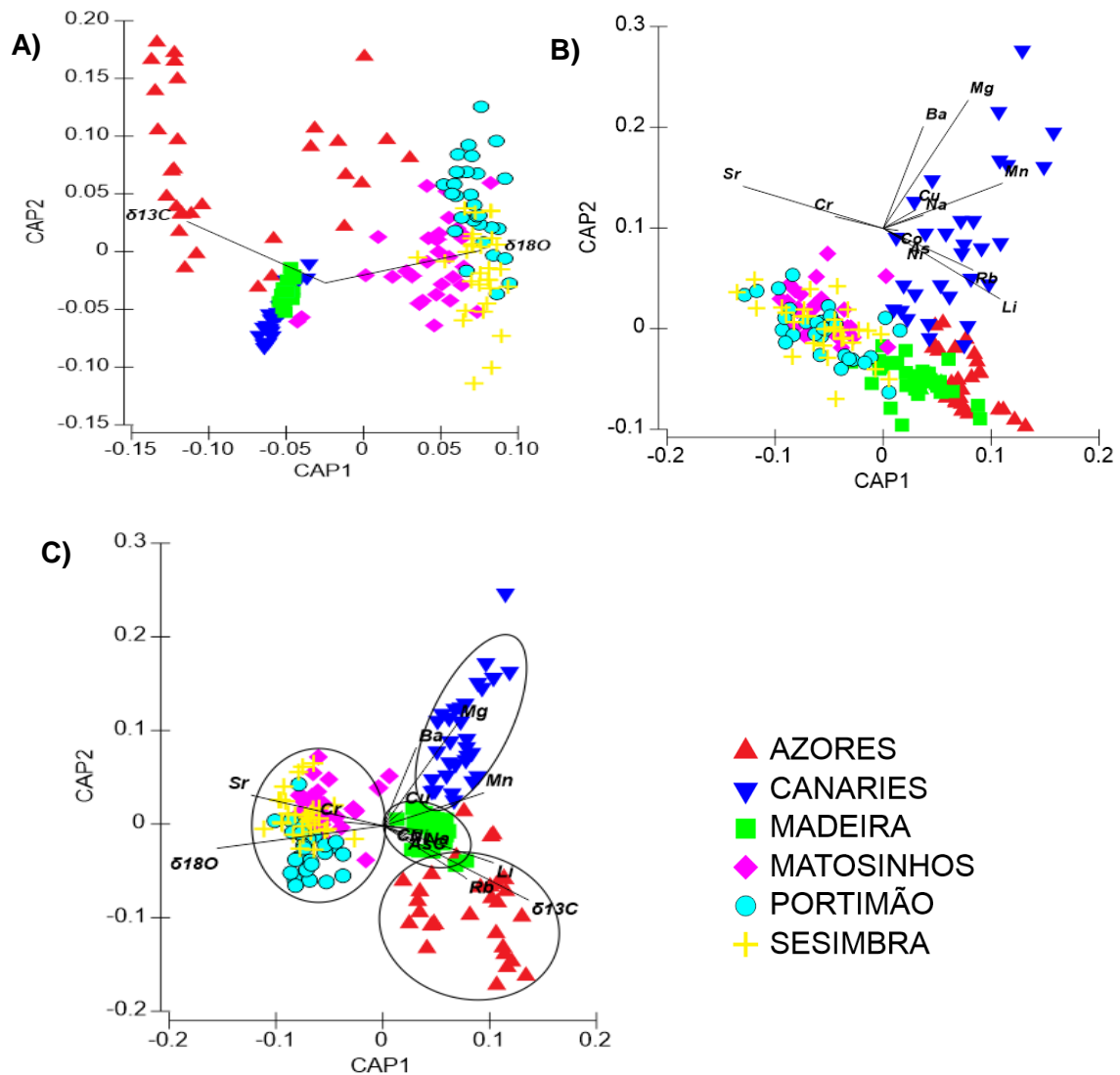


Figure 18: Canonical analysis of principal coordinates (CAP) plots for isotopic (A), elemental (B), and both elemental + isotopic (C), of the otolith of *Scomber colias*, respectively.

5. DISCUSSION

Although not fully understood, the otolith form could provide a phenotypic basis for separating the fish populations, considering that the otolith morphology varies geographically according to the effects of genetic variation and local environmental factors (Cardinale et al. 2004).

The results of otolith shape analysis showed some variations between sampling locations, but exhibited a high overlap of individuals especially when shape indices are

analysed separately. The EFD alone proved to be more useful than SI for discriminating between fish belonging to different sampling locations, while the SI were more valuable for explaining which otolith characteristics varied between locations. For example, samples from the Madeira were highly discriminated based on the RO and RE. Samples from the Sesimbra were more influenced by EL.

The data showed that the combination of both EFD and SI slightly improved the overall reclassification success. The LDFA based on SI, had little overall success in discriminating among samples (27%) and moderate overall success based on EFD (50%) and SI + EFD (51%). Data show that misclassification was mainly among the individuals within two groups, the islands (Azores, Canaries and Madeira) and the Portugal mainland (Matosinhos, Portimão and Sesimbra), suggesting a discrete separation in these two groups, especially when the SI and EFD combined. These findings are corroborated by the visual inspection of DFA and CAP plots; a separation of the two main sampling regions, i.e., Canaries/Azores/Madeira and Portugal mainland. RE and RO were the most informative for the Canaries/Azores/Madeira and EL were the most informative for the Portugal mainland.

Probably differences in otolith shape between the islands and Portugal mainland could be attributed to different environmental conditions, such as water temperature and feeding regimes, which in turn is related to the species growth rate and consequently affects the shape of otoliths (Mille et al., 2016; Campana and Neilson, 1985).

The body morphological data revealed significant differences for all morphometric measures between groups. The multivariate analysis showed a clear distinction between Canaries and the other regions. A distinction is also observed between the samples from the Portuguese coast (Matosinhos, Portimão and Sesimbra) and the Azores/Madeira. Thus, body morphometry suggests three main populations, i.e., Canaries, Azores/Madeira and Portugal mainland.

The length of the dorsal fin and distance from origin of dorsal fin to origin of anal fin were bigger in the samples from Canaries; the height and length of the fish were bigger in the samples from Azores/Madeira; and the head length and mouth size were larger in the samples from Portugal mainland.

The differences in morphometric characteristics of *S. colias* between regions may be related to a migration feeding strategy (Roldán et al., 2000). In a study carried out by Castro (1993) with *S. colias* from Canaries, affirms that probably the carrying capacity is limited of the shallow coastal waters, in combination with other factors, forcing juveniles

S. colias to migrate offshore, where they can find enough food. Fish are known to exhibit a large component of environmentally induced morphological variation which might reflect different feeding strategies and/or developmental environments (Allaya et al., 2013). The hereby observed regional variation, mainly on head width and mouth size, may be individual feed adaptations to different environments. In a study done with the chub mackerel species in the Black, Marmara, Aegean and Mediterranean Seas also identified regional differences between the size of the head and the mouth attributed to growth responses to the differing habitats arising from oceanographic and ecological conditions (Erguden et al., 2009). Other recent study of the chub mackerel morphometry in the southwest Atlantic Ocean reported that greater head length but lower mouth width and interorbital length were the primary characteristic difference between the stocks (Roldán et al., 2000). Other study also reported that the increase in the length of the body of chub mackerel was correlated with decreasing head size, which is related to a migration feeding strategy (Perrotta et al., 1999).

In relation to otolith elemental and isotopic signatures (Sr:Ca, Li:Ca, Mg:Ca, Mn:Ca, Ba:Ca, $\delta^{13}\text{C}$ and $\delta^{18}\text{O}$) for the otoliths from *S. colias* were within the range values found for other marine fishes (e.g., Correia et al., 2011a; Silva et al., 2011; Correia et al., 2012; Daros et al., 2016; Moreira et al., 2018). The elemental and isotopic signatures data mainly showed a significant variation in the chemical composition of the whole otoliths among the Atlantic oceanic islands and Portugal mainland sampling locations. QDFA of the both elemental and isotopic signatures showed a general trend suggesting a clear discrimination amongst the four main regions: Canaries, Azores, Madeira, and Portugal mainland. This regional variation was largely driven by Sr:Ca, Li:Ca, Mn:Ca, Mg:Ca, Rb:Ca, Ba:Ca, $\delta^{13}\text{C}$ and $\delta^{18}\text{O}$. This discrimination suggesting low levels of connectivity between these fishing grounds and suggests the existence of 4 populations-units for stock management purposes.

The physic-chemical properties of the environment, fish physiology and feeding regime are among the factors that can influence the potential incorporation of elements in the otoliths (Campana et al., 2000).

Individuals captured in the Portuguese mainland coastal water had higher Sr concentrations than the oceanic islands. Recently Moreira et al. (2018) also recorded lower Sr concentrations in the otoliths of *Trachurus picturatus* from islands (Canaries, Azores, Madeira) than in the Portugal mainland. Sr is a trace element that is noticeably influenced by its ambient concentration (Bath et al., 2000; Elsdon and Gillanders, 2004).

Patterns Sr incorporation in otoliths is positively influenced by temperature and positive correlation between otolith Sr:Ca and water salinity (Campana et al., 2000; Bath et al., 2000). This lower Sr otolith content in the islands may have occurred due to higher temperature and low salinity in water (Diop et al., 2014). The lower Sr concentration of the Azores can be explained by higher temperature or low-salinity water advected by upwelling filaments generated in the upwelling area (Barton et al., 1998).

Concerning the Li content in otoliths, a higher concentration was recorded in otoliths from the islands. Moreira et al. (2018) also recorded higher Li concentrations in the otoliths of *T. picturatus* from the islands (Canaries, Azores, Madeira) than in the Portugal mainland. The ratio Li:Ca increases with salinity (Hicks et al., 2010). The Canary Islands are influenced by Canary Currents (Moreira et al., 2018). These currents are expected to cause some degree of instability and could be the reason for the lower Li concentration in Canaries, when compared to the other islands (Sala et al., 2013). Li presents a high success rate for distinguishing fish reared at different salinities, as the ratio Li:Ca increases with salinity (Hicks et al., 2010), however the pathway Li into the otolith structure is not well understood (Correia et al., 2011a).

Regarding Ba the values obtained were higher in the Canaries than all other regions sampling. Upwelling processes and terrestrial sources are often linked to variations in water chemistry (Hamer et al., 2006) and Ba seems to be a reliable indicator of these changes (Moreira et al., 2018). Thus, the combined effect of the freshwater input from the surrounding rivers along with upwelling and terrestrial enrichment may explain these results (Hamer et al., 2006; Hicks et al., 2010). Thereover, the effect in the Canaries can be explained by the higher precipitation and rivers of the Africa coast and/or by upwelling (Diop et al., 2014; Barton et al., 1998).

Variation in the otolith Mn and Mg concentrations were higher from Canaries. Rb concentrations were higher from Azores. In the literature, there is no clear evidence of links between the variation in the otolith concentrations of Rb, Mn and Mg and ambient concentrations.

The lower $\delta^{18}\text{O}$ values were found at the islands. Moreira et al. (2018) also recorded lower $\delta^{18}\text{O}$ values in the otoliths of *T. picturatus* from the islands (Azores, Madeira) than in the Portugal mainland. The $\delta^{18}\text{O}$ composition in otoliths is highly influenced by temperature and salinity (Correia et al., 2011b). Assuming that in the study area the seawater $\delta^{18}\text{O}$ composition is homogenous, lower values of $\delta^{18}\text{O}$ would mean higher temperatures (Ashford and Jones, 2007). In general, the temperature of the

islands is larger than that of mainland Portugal, confirming the expected trend. In fact, the $\delta^{18}\text{O}$ values observed across the sampling area followed this expected trend, i.e., presenting higher values in the northern sampling locations (expected lower water temperatures, e.g., Sala et al., 2013) and decreasing towards the south (expected higher water temperatures, e.g., Sala et al., 2013). However, Matosinhos, the site located at a higher latitude in the Portugal mainland, showed a lower value of $\delta^{18}\text{O}$ when compared to with the other sites in the Portuguese coast. One possible reason for this may be the presence of the river Douro close to the Matosinhos sampling location, with probably derived from emissions from the city of Porto through sewage, agricultural waste or due to the extensive river use by tourism and commercial boats (Netzbund 2006). The large input of freshwater from the Douro River is most likely to explain this unexpected low value, as shown by previous studies for other fishes (Correia et al., 2011a; Carvalho et al., 2017).

The lower $\delta^{13}\text{C}$ values were found at the Portugal mainland. The $\delta^{13}\text{C}$ composition in otoliths is influenced by ontogenetic changes in trophic levels (i.e., fish diet, growth, and metabolism), that are considered the main endogenous factors that affect the incorporation of $\delta^{13}\text{C}$ into the otolith's aragonitic structure (Gillooly et al., 2001; Gao et al., 2004). However, the Atlantic islands, exhibit typically low productive (oligotrophic) open ocean waters (Martins et al., 2007). The results can be explained by islands upwelling, important because it increases food availability, but also enables the retention of larvae and juveniles in the region, which accentuates the higher values of $\delta^{13}\text{C}$ found in the otoliths (Roy et al., 1989; Sala et al., 2013). In a study carried out by Moreira (2018), it obtained higher results in the Islands than in Continental Portugal, unlike in the present study, where it explained its results by a southward coastal upwelling in summer, parallel to the Iberian coast, as a result of the Portuguese Current.

Other factors influencing the chemical composition of otoliths may be directly associated with fish, such as bioecology (feeding, physiology, reproduction), genetics and evolutionary history (Volpedo and Vaz-dos-Santos, 2015).

The multivariate analysis of the otolith isotopic and elemental fingerprints showed clear separation of the four main sampling regions, i.e., Canaries, Azores, Madeira and Portugal mainland. Mg:Ca and Ba:Ca were the most informative for the Canaries, Rb:Ca, $\delta^{13}\text{C}$ were the most informative for the Azores, Mn:Ca and Li:Ca were the most informative for the Madeira and Sr:Ca and $\delta^{18}\text{O}$ were the most informative for the Portugal mainland. Within the fishing region of Portugal mainland, differences were found

mainly between Matosinhos and Portimão, with samples from Sesimbra overlapping these two sites.

Knowing that the otolith shape analysis was able to separate two groups, the body morphometry able to separate three groups, and the otolith chemistry was able to separate four groups, so probably the otolith chemistry was the most efficient tool for stock discrimination purposes. Furthermore, although the data showed some regional differences in the otolith shape analysis and body morphometric, these differences are not fully conclusive, since LDFA and CAP plots were unclear to isolate the different population units. Moreover, the sites on the Portuguese mainland coast exhibited a high overlap of individuals suggesting a high connectivity at short geographic scales.

The isolation among the main four regions probably resulted from genetic and environmental differences among samples locations that could have affected the chemistry of otoliths and may be indicative of spatial stock structure.

6. CONCLUSION

Otolith chemistry is a competent tool to study fish ecology, providing useful information about population structure, movement patterns and habitat connectivity (Correia et al., 2014; Daros et al. 2016a; Moreira et al. 2018). In addition, the body morphometrics is also useful to discriminate fish stock structure of various exploited marine fish species (Erguden et al., 2009; Allaya et al., 2013; Kaouèche et al., 2017). Besides this, otolith shape analysis has proven successful in resolving fish stock structure in high gene flow systems, when environmental heterogeneity exists (Tuset et al. 2003; Stransky et al., 2008; Bacha et al. 2014).

Rules and policies must be more monitored to should ensure good practices. The sustainable fisheries management and of the biological renewable resources is very important for determine the number or weight of a species that can be removed from the stock, without impacting the long-term stability of the population (NOAA, 2014), and for the populations of organisms grow and replace themselves (Holt, 2011).

Body morphometric, otolith shape and chemical analysis have proven useful here to unravel stock delineation of *S. colias*, but further investigation into the population structure, fish movement and habitat connectivity is still needed. This study showed that using shape otolith was separation two groups (Islands and Portugal mainland), using

body morphometric was separation three groups (Canaries, Azores/Madeira and Portugal mainland) and using otolith chemistry was separation four groups (Canaries, Azores, Madeira and Portugal mainland). So, using otolith chemistry was most efficient tool for separation of the stocks, distinguishing four populations units.

Ideally stock identification based on morphological characters must be confirmed by genetic evidence to verify that the phenotypic differences reflect some degree of reproductive isolation rather than simply environmental differences (Ergüden et al., 2009).

At present, it is considered the existence of a single stock of *S. colias* in the Northeast Atlantic based on mtDNA analysis (Scoles et al., 1998; Zardoya et al., 2004). The present work opens a new debate regarding the possibility of different population units mainly in the Atlantic islands. In general, he noticed the existence of four groups formed, the islands (Canaries, Madeira and Azores) and Portugal mainland. So, the data suggest the possibility for *S. colias* in the NE Atlantic regarded as four independent populations units and thus be treated separately in terms of fisheries management.

Moreover, this study also highlights the need of a holistic approach when using phenotypic tags to properly infer about the population structure in fish. Because of the complexity and requirement for a multi-faceted approach to delineate a fish stock, future works should focus on a larger geographic area, besides the use of other natural tags, such as genetic markers.

7. FINANTIAL SUPPORT

I would also like to acknowledge the partially supported by the NORTE-01-0145-FEDER-000035 (MARINFO) and the Strategic Funding UID/Multi/ 04423/2013 through national funds provided by Foundation for Science and Technology (FCT) and European Regional Development Fund (ERDF), in the framework of the programme PT2020.

8. REFERENCES

Allaya, H., Hattour, A., Hajjej, G., Trabelsi, M., 2013. Biologic characteristics of *Scomber japonicus* (Houttuyn, 1782) in Tunisian waters (Central Mediterranean Sea). African Journal of Biotechnology. 12(20), 3040–3048.

Aquamaps., 2016. Reviewed Native Distribution Map for *Scomber colias* (Atlantic chub mackerel), with modelled year 2100 native range map based on IPCC A2 emissions scenario. www.aquamaps.org, version of Aug. 2016. Web. Accessed 4 Jun. 2018.

Ashford, J., Jones, C., 2007. Oxygen and carbon stable isotopes in otoliths record spatial isolation of Patagonian toothfish (*Dissostichus eleginoides*). Geochimica Cosmochimica Acta. 71, 87–94.

Bacha, M., Jemaa, S., Hamitouche, A., Rabhi, K., Amara, R., 2014. Population structure of the European anchovy, *Engraulis encrasicolus*, in the SW Mediterranean Sea, and the Atlantic Ocean: evidence from otolith shape analysis. ICES Journal Marine Science. 71, 2429–2435.

Baird, D. 1978. Food of the Mackerel *Scomber japonicus* from Western Cape waters. Fishery Bulletin of South Africa. 10, 62–68.

Barton, E.D., Arístegui, J., Tett, P., Cantón, M., García-Braun, J., Hernández-León, S., Nykjaer, L., Almeida, C., Almunia, J., Ballesteros, S., Basterretxea, G., Escánez, J., García-Weill, L., Hernández-Guerra, A., López-Laatzén, F., Molina, R., Montero, M.F., Navarro-Pérez, E., Rodríguez, J.M., van Lenning, K., Vélez, H., Wild, K., 1998. The transition zone of the Canary Current upwelling region. Progress Oceanography. 41, 455–504.

Bath, G.E., Thorrold, S.R., Jones, C.M., Campana, S.E., McLaren, J.W., Lam, J.W.H., 2000. Strontium and barium uptake in aragonitic otoliths of marine fish. Geochimica Cosmochimica Acta. 64, 1705–1714.

Cabral, H.N., Marques, J.F., Rego, A.L., Catarino, A.I., Figueiredo, J., Garcia, J., 2003. Genetic and morphological variation of *Synaptura lusitanica* Capello, 1868, along the Portuguese coast. *Journal of Sea Research*. 50, 167–175.

Campana, S.E., Neilson, J.D., 1985. Microstructure of fish otoliths. *Canadian Journal of Fisheries and Aquatic Sciences*. 42 (5), 1014-1032.

Campana, S.E., Casselman, J.M., 1993. Stock discrimination using otolith shape analysis. *Canadian Journal of Fisheries and Aquatic Sciences*. 50, 1062-1083.

Campana, S.E., 1999. Chemistry and composition of fish otoliths: pathways, mechanisms and applications. *Marine Ecology Progress Series*. 188, 263–297.

Campana, S.E., Chouinard, G.A., Hanson, J.M., Fréchet, A., Bratley, J., 2000 Otolith elemental fingerprints as biological tracers of fish stocks. *Fisheries Research*, 46, 343–357.

Campana, S. E., Stanley, R. D., Wischiowski, S., 2003. Suitability of glycerin-preserved otoliths for age validation using bomb radiocarbon. *Journal of Fish Biology*. 63, 848–854.

Cardinale, M., Doering-Arjes, P., Kastowsky, M., Mosegaard, H., 2004. Effects of sex, stock, and environment on the shape of known-age Atlantic cod (*Gadus morhua*) otoliths. *Canadian Journal of Fisheries and Aquatic Sciences*. 61, 158-167.

Carvalho, M.G., Moreira, C., Cardoso, J.F.M.F., Brummer, G.A., Gaever, P., Veer, H.W., Queiroga, H., Santos, P.T., Correia, A.T., 2017. Movement, connectivity and population structure of the intertidal fish *Lipophrys pholis* as revealed by otolith oxygen and carbon stable isotopes. *Marine Biology Research*. 13(7), 764-773.

Carvalho, N., Perrota R.G., Isidro, E.J., 2002. Age, growth and maturity in the chub mackerel (*Scomber japonicus* Houttuyn, 1782) from the Azores. *Arquipélago. Life and Marine Sciences*. 19A, 93-99.

Castro, J.J., 1993. Feeding ecology of chub mackerel *Scomber japonicus* in the Canary Islands area. South African Journal of Marine Science. 13(1), 323-328.

Castro, J. J., Hernández-García, V., 1995. Ontogenetic changes in mouth structures, foraging behaviour and habitat use of *Scomber japonicus* and *Illex condetti*. International Symposium on middle-sized pelagic fish. Scientia Marina. 59(3-4), 347-355.

Castro-Hernández, J. J., Santana-Ortega, A. T., 2000. Synopsis of biological data on the chub mackerel (*Scomber japonicus*, 1782). FAO Fisheries Synopsis. Roma, n.157, 77pp.

Catanese, G., Manchado, M., Infante, C., 2010. Evolutionary relatedness of mackerels of the genus *Scomber* based on complete mitochondrial genomes: Strong support to the recognition of Atlantic *Scomber colias* and Pacific *Scomber japonicus* as distinct species. Gene. 452, 35-43.

Collette, B.B., Nauen, C.E., 1983. Scombrids of the world. FAO Fisheries Synopsis. Rome, n.125, 137 pp.

Collette, B.B., 1986. Scombridae. In: Whitehead, P.J.P., Bauchot, M.L., Hureau, J.C., Nielsen, J., Tortonese, E. Fish of the North-eastern Atlantic and the Mediterranean. UNESCO, Paris, 981-997.

Correia, A.T., Pipa, T., Gonçalves, J. M. S., Erzini, K., Hamer, P. A., 2011a. Insights into population structure of *Diplodus vulgaris* along the SW Portuguese coast from otolith elemental signatures. Fisheries Research. 111(1-2), 82-91.

Correia, A.T., Barros, F., Sial, A. N., 2011b. Stock discrimination of European conger eel (*Conger conger* L.) using otolith stable isotope ratios. Fisheries Research, 108(1), 88-94.

Correia, A.T., Gomes, P., Gonçalves, J.M.S., Erzini, K., Hamer, P.A., 2012. Population structure of the black seabream *Spondyliosoma cantharus* along the south-west Portuguese coast inferred from otolith chemistry. Journal of Fish Biology. 80, 427-443.

Correia, A.T., Hamer, P., Carocinho, B., Silva, A., 2014. Evidence for meta-population structure of *Sardina pilchardus* in the Atlantic Iberian waters from otolith elemental signatures of a strong cohort. *Fisheries Research*. 149, 76–85.

Correia, C. 2016. Study of Atlantic chub mackerel's (*Scomber colias*, Gmelin, 1789) landings evolution in Portugal: importance for purse seine fleet. Master thesis. Evora University. 87 p.

Couto C., Pinto I., Rocha M.J., Almeida A., 2010. Spatial and temporal monitorization of metals in Leça river (Portugal). SETAC Europe 20th Annual Meeting. Seville. 62, 23-27.

Daros, F.A., Spach, H.L., Sial, A.N., Correia, A.T., 2016. Otolith fingerprints of the coral reef fish *Stegastes fuscus* in southeast Brazil: a useful tool for population and connectivity studies. *Regional Studies in Marine Science*. 3, 262–272.

Diop, S., Fabres, F., Pravettoni, R., Barousseau, J.P., Descamps, C., Ducrotoy, J.P., 2014. The western and central africa land–sea interface: a vulnerable, threatened, and important coastal zone within a changing environment. *The Land/Ocean Interactions in the Coastal Zone of West and Central Africa*. Part of the Series *Estuaries of the World*. pp. 1–8.

DGRM., 2018. Recursos da Pesca. Série Estatística, 30 A-B. www.dgrm.mm.gov.pt, version of 2017. Web. Accessed 29 Aug. 2018.

Dwivedi, A.K., Dubey, V.K., 2012. RETRACTED ARTICLE: Advancements in morphometric differentiation: a review on stock identification among fish populations. *Fish Biology and Fisheries*, 23(1), 23–39.

Erguden, E., Öztürk, B., Erdogan, Z.A., Turan C., 2009. Morphologic structuring between populations of chub mackerel *Scomber japonicus* in the Black, Marmara, Aegean, and northeaster Mediterranean Seas. *Fisheries Science*. 75, 129–135.

Elsdon, T.S., Gillanders, B.M., 2004. Fish otoliths chemistry influenced by exposure to multiple environmental variables. *Journal of Experimental Marine Biology Ecology*. 313, 269–284.

FAO., 2016. FAO yearbook: Estadísticas de pesca y acuicultura 2016. Rome. 104pp.

Ferguson, G.J., Ward, T.M., Gillanders, B.M., 2011. Otolith shape and elemental composition: complementary tools for stock discrimination of mullet (*Argyrosomus japonicus*) in southern Australia. *Fisheries Research*. 110, 75-83.

Gao, Y., Joner, S.H., Svec, R.A., Weinberg, K.L., 2004. Stable isotopic comparison in otoliths of juvenile sablefish (*Anoplopoma fimbria*) from waters off the Washington and Oregon coast. *Fisheries Research*. 68, 351–360.

Gerard, T., Muhling, B., 2010. Variation in the isotopic signatures of juvenile gray snapper (*Lutjanus griseus*) from five southern Florida regions. *Fishery Bulletin*. 108, 98-105.

Gillooly, J.F., Brown, J.H., West, G.B., Savage, V.M., Charnov, E.L., 2001. Effects of size and temperature on metabolic rate. *Science*. 293, 2248–2251.

Gobierno de Canarias., 2018. Observaciones del Gobierno de Canarias al libro verde sobre la reforma de la política pesquera común. www.ec.europa.eu. Accessed 12 Sep. 2018.

Green, B.S., Mapstone, B.D., Carlos, G. Begg, G.A., 2009. Tropical fish otoliths information for assessment, management and ecology. *Springer Science + Business Media B*. 11, 1571-3075.

Hamer, P.A., Jenkins, G.P., Coutin, P., 2006. Barium variation in *Pagrus auratus* (Sparidae) otoliths: a potential indicator of migration between an embayment and ocean waters in south-eastern Australia. *Estuarine, Coastal and Shelf Science*. 68, 686–702.

Hicks, A.S., Closs, G.P., Swearer, S.E., 2010. Otolith microchemistry of two amphidromous galaxiids across an experimental salinity gradient: A multi-element approach for tracking diadromous migrations. *Journal of Experimental Marine Biology and Ecology*. 394, 86–97.

Holt, J., Butenschon, M., Wakelin, S.L., Artioli, Y., 2011. Oceanic controls on the primary production of the northwest European continental shelf under recent past and potential future conditions. *Biogeosciences. Discussions*. 8, 1–40.

Hunter, J. R., Kimbrell, C. A., 1980. Early life history of pacific mackerel, *Scomber japonicus*. Southwest, Fisheries Center La Jolla Laboratory, National Marine Fisheries Service, NOAA, P.O. Box 271, La Jolla, CA 92038. Fishery bulletin: vol. 78, n. 1.

ICES, 2015. Report of the Workshop on Age Reading of Chub Mackerel (*Scomber colias*) (WKARCM), Lisbon, 02-06 November 2015. ICES CM 2015\SSGEIOM:11.

Infante, C., Blanco, E., Zuasti, E., Crespo, A., Manchado, M., 2007. Phylogenetic differentiation between Atlantic *Scomber colias* and Pacific *Scomber japonicus* based on nuclear DNA sequences. *Genetica* 130, 1–8.

Jemaa, S., Bacha, M., Khalaf, G., Dessailly, D., Rabhi, K., Amara, R., 2015. What can otolith shape analysis tell us about population structure of the European sardine, *Sardina pilchardus*, from Atlantic and Mediterranean waters? *Journal Sea Research*. 96, 11-17

Kaouèche, M., Bahri-Sfar, L., Hammami, Ibtissem., Hassine, O.K.B., 2017. Morphometric variations in white seabream *Diplodus sargus* (Linneus, 1758) populations along the Tunisian coast. *Oceanologia*, 59: 129 - 138.

Kiparissis, S., Tserpes, G., Tsimenidis, N., 2000. Aspects on the demography of Chub Mackerel (*Scomber japonicus* Houttuyn, 1782) in the Hellenic Seas. *Belgian Journal of Zoology*. 130(1), 3-7.

Knutsen, H., Jorde, P.E., André, C., Stenseth, N.C., 2003. Fine-scaled geographical population structuring in a highly mobile marine species: The Atlantic cod. *Molecular Ecology*. 12, 385– 394.

Kuhl, F.P., Giardina, C.R., 1982. Elliptic Fourier features of a closed contour. *Computer Graphics and Image Processing*. 18, 236-258.

Lockwood S.J. 1988. The mackerel, its biology, assessment and the management of a fishery. Fishing News Books. Farnham, Surrey, UK, 181 p.

Lorenzo, J.M., 1992. Crecimiento de la cabala *Scomber japonicus* Houttuyn, 1782 em aguas del Archipélago Canario. Ph.D. thesis, Univ. Las Palmas de Gran Canaria, 199pp. [in Spanish]

Lorenzo, J.M., Pajuelo J.M.G., Ramos A.G., 1995. Growth of the chub mackerel *Scomber japonicus* (Pisces: Scombridae) off the Canary Island. *International Symposium on middle-sized pelagic fish*. Scientia Marina. 59(3-4), 287-291.

Lucio, P., 1997. Biological Aspects of Spanish (Chub) Mackerel (*Scomber japonicus*, Houttuyn, 1782) in the Bay of Biscay from the Basque Country Catches. *International Council for the Exploration of the Sea Conference and Meeting (CM) Document 1997/BB:10*, 31 pp.

Martins, M.M., 1996. New biological data on growth and maturity of Spanish mackerel (*Scomber japonicus*) off the Portuguese coast (ICES Division IX a). *International Council for the Exploration of the Sea Conference and Meeting (CM) Document 1996/H:23*, 17 pp.

Martins, M.M., Cardador, F., 1996. Abundance and distribution pattern of Spanish Mackerel (*Scomber japonicus*) and Mackerel (*Scomber scombrus*) in the Portuguese continental waters (ICES DIV. IXa). *Pelagic Fish Committee, ICES C.M.1996/H:24*.

Martins, M.M., 2007. Growth variability in Atlantic mackerel (*Scomber scombrus*) and Spanish mackerel (*Scomber japonicus*) off Portugal. ICES Journal of Marine Science. 64, 1785–1790.

Martins, M.M., Skagen, D., Marques, V., Zwolinski, J., Silva A., 2013. Changes in the abundance and spatial distribution of the Atlantic chub mackerel (*Scomber colias*) in the pelagic ecosystem and fisheries off Portugal. Scientia Marina. 77(4), 551-563.

Mille, T., Ernande, B., Pontual, H., Villanueva, C., Mahé, K., 2016. Sources of otolith morphology variation at the intra-population level: directional asymmetry and diet. SFI days, Marseille, France.

Miller, J.A., 2009. The effects of temperature and water concentration on the otolith incorporation of barium and manganese in black rockfish *Sebastes melanops*. J. Fish Biology. 75, 39–60.

Moreira, C., Froufe, E., Sial, A.N., Caeiro, A., Vaz-Pires, P., Correia, A.T., 2018. Population structure of the blue jack mackerel (*Trachurus picturatus*) in the NE Atlantic inferred from otolith microchemistry. Fisheries Research. 197, 113-122.

Navarro, M.R., Villamor B., Landa J., Hernandez C., 2014. Reproductive characteristics and body condition of chub mackerel (*Scomber colias*) in the south of Bay of Biscay, 2011-2013. XIV International Symposium on Oceanography of the Bay of Biscay.

Nespereira, J.M.L., Pajuelo J.M.G., 1993. Determinación de la talla de primera madurez sexual y período reproductivo de la caballa (*Scomber japonicus* Houttuyn, 1782) de las islas Canarias. Boletín del Instituto Español de Oceanografía 9 (1): 15-21. [in Spanish]

Nespereira, J.M.L., Pajuelo J.M.G., 1996. Determinación del crecimiento de la caballa *Scomber japonicus* (Houttuyn, 1782) de las islas Canarias a través del análisis de las frecuencias de tallas. Boletín Instituto Español de Oceanografía 12(2): 83-90. [in Spanish]

Netzband, A., 2006. Sediment management: an essential element of river basin management plans. Report on the SedNet Round Table Discussion, Venice.

NOAA., 2014. Status of Stocks 2014 – Annual report to Congress on the Status of U.S. Fisheries. www.nmfs.noaa.gov. Web. Accessed 19 Jun. 2018.

Perrotta R.G., Madirolas, A., Viñas, M.D., Akselman, R., Guerrero, R., Sánchez, F., López, F., Castro Machado, F., Macchi, G., 1999. La caballa (*Scomber japonicus*) y las condiciones ambientales en el área bonaerense de “El Rincón”. INIDEP Inf Téc. 26, 1–29

Perrota, R.G., Carvalho, N., Isidro, E., 2005. Comparative study on growth of chub mackerel (*Scomber japonicus* HOUTTUYN, 1782) from three different regions: NW Mediterranean, NE and SW Atlantic. Revista de Investigacion y Desarrollo Pesquero. Nº 17, 67-79.

Patterson, H.M., Thorrold, S.R., Shenker, J.M., 1999. Analysis of otolith chemistry in Nassau grouper (*Epinephelus striatus*) from the Bahamas and Belize using solution based ICP-MS. Coral Reefs. 18, 171–178. [in Spanish]

Poper, A.N., Ramcharitar, J., Campana, S.E., 2005. Why otoliths? Insights from inner ear physiology and fisheries biology. Marine and Freshwater Research. 56, 497–504.

Reist, J.D., 1985. An empirical evaluation of several univariate methods that adjust for size variation in morphometric data. Canadian Journal of Zoology. 63(6), 1429–1439.

Rohlf, F.J., Slice, D., 1990. Extensions of the Procrustes method for the optimal superimposition of landmarks. Systematic Zoology. 39, 40–59.

Roldán, M.I., Perrotta, R.G., Cortey, M., Pla, C., 2000. Molecular and morphologic approaches to discrimination of variability patterns in chub mackerel, *Scomber japonicus*. Journal of Experimental Marine Biology and Ecology. 253, 63–74.

Rooker, J.R., Zdanowicz, V.S., Secor, D.H., 2001. Chemistry of tuna otoliths: assessment of base composition and postmortem handling effects. *Marine Biology*. 139, 35–43.

Roy, C.P., Cury, P., Fontana, A., Belvèze, H., 1989. Stratégies spatio-temporelles de la reproduction des clupéidés des zones d'upwelling d'Afrique de l'Ouest [Spatio-temporal reproductive strategies of the clupeoids in West African upwelling ares]. *Aquatic Living Resources*. 2, 21–29.

Sala, I., Caldeira, R.M.A., Estrada-Allis, S.N., Froufe, E., Couvelard, X., 2013. Lagrangian transport pathways in the northeast Atlantic and their environmental impact. *Limnology and Oceanography. Fluids Environments*. 3, 40–60.

Secor, D.H., Dean, J.M., Laban, E.H., 1992. Otolith removal and preparation for microstructural examination. In: Stevenson, D.K., Campana, S.E. *Otolith Microstructure Examination and Analysis*. Canadian Special Publication of Fisheries and Aquatic Sciences. 117, 19–57.

Scoles, D.R., Collette, B.C., Graves, J.E., 1998. Global phylogeography of mackerels of the genus *Scomber*. *Fisheries Bulletin*. 96, 823–842.

Silva, M.N.G., 1993. Aspectos da Biologia da Cavala, *Scomber japonicus* (Houttuyn, 1782) da Madeira. Relatório de Estágio Profissionalizante da Licenciatura em recursos Faunísticos e Ambiente. Faculdade de Ciências da Universidade de Lisboa. 143 pp. [in Portuguese]

Silva, D.M., Santos, P., Correia, A.T., 2011. Discrimination of *Trisopterus luscus* stocks in northern Portugal using otolith elemental fingerprints. *Aquatic Living Resources*. 24, 85–91.

Stransky, C., Murta, A.G., Schlickeisen, J., Zimmermann, C., 2008. Otolith shape analysis as a tool for stock separation of horse mackerel (*Trachurus trachurus*) in the Northeast Atlantic and Mediterranean. *Fisheries Research*. 89, 159–166.

Strauss, R.E., Bookstein, F.L., 1982. The truss: body form reconstruction in morphometrics. *Systematic Zoology*. 31 (2), 113–135.

Thorrold, S.R., Campana, S.E., Jones, C.M., Swart, P.K., 1997. Factors determining $\delta^{13}\text{C}$ and $\delta^{18}\text{O}$ fractionation in aragonite otoliths of marine fish. *Geochim. Cosmochim. Acta*. 61, 2909–2919

Tuset, V.M., Lozano, I.J., Gonzalez, J.A., Pertusa, J.F., Garcia-Diaz, M.M., 2003. Shape indices to identify regional differences in otolith morphology of comber *Serranus cabrilla* (L., 1758). *Journal of Applied Ichthyology*. 19, 88-93.

Vasconcelos, J., 2006. Contribuição para o conhecimento da biologia da cavala, *Scomber japonicus* Houttuyn, 1782 do Arquipélago da Madeira. PhD Tesis, Universidade da Madeira. [in Portuguese]

Vasconcelos, J., Dias M.A., Faria G., 2011. Age and growth of the Atlantic chub mackerel *Scomber colias* Gmelin, 1789 off Madeira Island. *Arquipelago. Life and Marine Sciences* 28, 57-70.

Vasconcelos, J., Afonso-Dias M., Faria G., 2012. Atlantic chub mackerel (*Scomber colias*) spawning season, size and age at first maturity in Madeira waters. *Arquipelago. Life and Marine Sciences* 29, 43-51.

Velasco, E.M., Arbol, J.D., Baro, J., Sobrino, I., 2011. Age and growth of the Spanish chub mackerel *Scomber colias* off southern Spain: a comparison between samples from the NE Atlantic and the SW Mediterranean. *Revista de Biología Marina y Oceanografía*, 46, 27–34.

Villamor, B., Carrera, P., Castro, J., Ramos, F., Velasco, F., Sobrino, I., Navarro, M.R., Gancedo, R., Hernandez, C., Marín, M., Blanco, M., Tornero, J., Burgos, C., 2017. The Chub Mackerel (*Scomber colias*) in the Atlantic Spanish Waters (ICES Divisions 8.c and 9.a): Biological, fishery and survey data. Working Document to WGWIDE, 61pp.

Volpedo, A.V., Vaz-dos-Santos, A.M., 2015. Métodos de estudios con otolitos: principios y aplicaciones/ Métodos de estudos com otólitos: princípios e aplicações. 1ª ed, edición bilingue, Ciudad Autónoma de Buenos Aires. [in Spanish]

Zardoya, R., Castilho, R., Grande, C., Favre-Krey, L., Caetano, S., Marcato, S., Krey, G., Paternello, T., 2004. Differential population structuring of two closely related fish species, the mackerel (*Scomber scombrus*) and the chub mackerel (*Scomber japonicus*), in the Mediterranean Sea. *Molecular Ecology*. 13, 1785–1798.

Whitehead, P.J.P., Bauchot, M.L., Hureau, J.C., Nielsen, J., Tortonese, E., 1984. Fishes of the North - eastern Atlantic and the Mediterranean. UNESCO, 2 Scombridae, 981-997.